Llorente-Ovejero, Alberto et al. '*Endocannabinoid and Muscarinic Signaling Crosstalk in the 3xTg-AD Mouse Model of Alzheimer's Disease*'. **Journal of Alzheimer's Disease**, vol. 64, no. 1, pp. 117-136, 2018. Copyright © 2018 The Authors published by IOS Press. DOI: 10.3233/JAD-180137.

Title page

Endocannabinoid and Muscarinic Signaling Crosstalk in the 3xTg-AD Mouse Model of Alzheimer's Disease

Alberto Llorente-Ovejero[1], Iván Manuel[1], Laura Lombardero[1], Maria Teresa Giralt[1], Catherine Ledent[2], Lydia Giménez-Llort[3], Rafael Rodríguez-Puertas[1]

[1]Department of Pharmacology, Faculty of Medicine and Nursing, University of the Basque Country (UPV/EHU), Bº Sarriena s/n, 48940 Leioa, Spain.

[2]Institut de Recherche Interdisciplinaire en Biologie Humaine et Moléculaire, Université Libre de Bruxelles, Brussels B-1070, Belgium.

[3]Department of Psychiatry and Forensic Medicine, Institut de Neurociències, Universitat Autònoma de Barcelona, 08193 Bellaterra, Spain.

Running title: **Cannabinoid/Muscarinic Signaling in 3xTg-AD**

*Corresponding author: Rafael Rodríguez-Puertas, Department of Pharmacology, Faculty of Medicine and Nursing, University of the Basque Country, E-48940 Leioa, Vizcaya, Spain. E-mail address: rafael.rodriguez@ehu.es. Tel.: +34-94-6012739; fax: +34-94-6013220.

Abstract

The endocannabinoid system, which modulates emotional learning and memory through CB_1 receptors, has been found to be deregulated in Alzheimer's disease (AD). AD is characterized by a progressive decline in memory associated with selective impairment of cholinergic neurotransmission. The functional interplay of endocannabinoid and muscarinic signaling was analyzed in seven-month-old 3xTg-AD mice following the evaluation of learning and memory of an aversive stimulus. Neurochemical correlates were simultaneously studied with both receptor and functional autoradiography for CB_1 and muscarinic receptors, and regulations at the cellular level were depicted by immunofluorescence. 3xTg-AD mice exhibited increased acquisition latencies and impaired memory retention compared to age-matched non-transgenic mice. Neurochemical analyses showed changes in CB_1 receptor density and functional coupling of CB_1 and muscarinic receptors to $G_{i/o}$ proteins in several brain areas, highlighting that observed in the basolateral amygdala. The subchronic (seven days) stimulation of the endocannabinoid system following repeated WIN55,212-2 (1 mg/kg) or JZL184 (8 mg/kg) administration induced a CB_1 receptor down-regulation and CB_1-mediated signaling desensitization, normalizing acquisition latencies to control levels. However, the observed modulation of cholinergic neurotransmission in limbic areas did not modify learning and memory outcomes. A CB_1 receptor-mediated decrease of GABAergic tone in the basolateral amygdala may be controlling the limbic component of learning and memory in 3xTg-AD mice. CB_1 receptor desensitization may be a plausible strategy to improve behavior alterations associated with genetic risk factors for developing AD.

Keywords**:** Alzheimer, 3xTg-AD, cholinergic, endocannabinoid, learning and memory, basolateral amygdala, autoradiography.

Abbreviations

2-AG: 2-arachidonoylglycerol; 3xTg-AD: Triple transgenic mice model; Aβ: Amyloid-β; AD: Alzheimer´s disease; AEA: anandamide; BLA: Basolateral amygdala; CB_1 receptor: Type-1 cannabinoid receptors; $CB_1^{-/-}$: CB_1 receptor knockout mice; eCB: Endocannabinoid; GAD65: Glutamic acid decarboxylase isoform 65kDa; GTPγS: Guanosine-5´-O-3-thiotriphosphate; mAChR: Muscarinic acetylcholine receptor; M_2 mAChR: Subtype-2 muscarinic receptor; MAGL: Monoacylglycerol lipase; Non-Tg: Non transgenic mice, VGLUT3: Vesicular glutamate transporter type 3.

Introduction

Alzheimer's disease (AD), the most common cause of dementia in the elderly, is characterized by a progressive impairment of memory and thinking skills, usually associated with agitation, psychosis, depression, apathy, disinhibition or anxiety. Most of these symptoms are dependent on the cholinergic deficit described in AD [1-2]. The cholinergic neurotransmission that controls learning and memory is specifically vulnerable in AD [3-8]. Impaired functionality of muscarinic receptors (mAChR) is found in areas that control cognitive processes, such as the amygdala and the hippocampus [8]. Different neuromodulators of the cholinergic system, including neurolipids, e.g. endocannabinoids (eCB), contribute to the alteration of cognitive and emotional processes [9]. Thus, a reduction of type-1 of cannabinoid receptors (CB_1) in different layers of the hippocampus is described at advanced Braak stages of the disease [10], while an increase in CB_1 receptor activity and density is found at early and moderated stages of AD [11]. Endogenous and exogenous cannabinoids seem to elicit modulatory effects in multiple AD-related processes, although the biochemical mechanisms need to be further investigated. Therefore, eCB system is foreseen as a novel potential therapeutic target to counteract the disease [12]. The triple transgenic mouse model of AD (3xTg-AD) shows impaired mAChR-mediated signaling in young animals (2-4 months). The cholinergic impairment is more evident at middle-aged mice (13-15 months), with a decrease in the activity of choline acetyltransferase. At 18-20 months the basal forebrain cholinergic neurons are affected together with hippocampal and cortical cholinergic neuritic dystrophy, in parallel with the progression of amyloid-β (Aβ) plaque formation [13-14]. Altered CB_1 receptor expression and functionality has also been described in the 3xTg-AD mice at different development stages (beginning at 4-6 months) [14-15]. These mice harbor APP_{Swe}, $PS1_{M146V}$, and tau_{P301L} transgenes and mimic several hallmarks of familial AD [16]. While Aβ and tau neuropathologies

develop in middle age (12 months), deficits in synaptic plasticity and cognition have earlier onsets, when intraneuronal accumulation of oligomeric-Aβ, is clearly established at 6 months of age [17]. So far, learning and memory deficits are apparent in several cognitive paradigms such as the passive avoidance, the novel-object recognition and the Morris water maze [18-19]. Fear and anxiety-like behaviors have also been shown in the open-field, the elevated plus maze, and the dark/light box [20-23]. Interestingly, in 6-month-old 3xTg-AD mice, the intraneuronal Aβ accumulation in the basolateral amygdala (BLA) has been shown to enhance innate and conditioned fear as assessed in fear conditioning paradigms [21].

The functional interplay of cannabinoid and muscarinic signaling was analyzed in relation to learning and memory of an aversive stimulus (step-through passive avoidance test). We examined the expression, neuroanatomical distribution, and functional coupling of CB_1 receptor and mAChR to $G_{i/o}$ proteins in seven-month-old 3xTg-AD mice and in age-matched non-transgenic (Non-Tg) counterparts, as well as following the subchronic eCB system activation.

Materials and methods

Animals

Seven-month-old male 3xTg-AD mice (n = 40) and age-matched Non-Tg mice (n = 18) were obtained from Universitat Autonòma de Barcelona, in collaboration with Dr Lydia Giménez Llort. The 3xTg-AD mice harboring $PS1_{M146V}$, APP_{Swe}, and Tau_{P301L} transgenes were genetically engineered as previously described (Oddo et al., 2003). Also, nine-week-old male $CB_1^{-/-}$ (n = 2) and $CB_1^{+/+}$ (n = 2) mice were used, provided by C. Ledent of the University of Brussels.

All the animals were housed (4-5 animals per cage) and maintained under standard laboratory conditions of 12 hours light-dark cycle with light from 8 am to 8 pm and availability of food/water *ad libitum*. All procedures were performed in accordance with European Directive 2010/63/EU and the Spanish National Guidelines for Animal Experimentation and the Use of Genetically Modified Organisms (Real Decreto 1205/2005) and 178/2004; Ley 32/2007 and 9/2003). Experimental protocols were approved by the local Committee for Animal Research at the University of the Basque Country (CEIAB/21/2010/Rodríguez-Puertas).

Drugs and treatments

R-(+)-[2,3-Dihydro-5-methyl-3-[(morpholinyl)methyl]pyrrolo[1,2,3-de]-1,4-benzoxazinyl]-(1-naphthalenyl)methanone mesylate (WIN55,212-2), (-)-*cis*-3-[2-Hydroxy-4-(1,1-dimethylheptyl)phenyl]-*trans*-4-(3-hydroxypropyl) cyclohexanol (CP55,940) and (2-Carbamoyloxyethyl) trimethylammonium chloride (carbachol) were acquired from Sigma-Aldrich (St Louis, MO, USA). 4-Nitrophenyl4-(dibenzo[d][1,3]dioxol-5-yl(hydroxy)methyl)piperidine-1-carboxylate (JZL184) and 5-(4-chloro-3-methylphenyl)-1-[(4-methylphenyl)methyl]-N-[(1S,2S,4R)-1,3,3-trimethylbicyclo[2.2.1]hept-2-yl]1pyrazole3-carboxamide (SR144528) were acquired from Cayman-Chemicals (MI, USA), and (Piperidin-1-yl)-5-(4-chlorophenyl)-1-(2,4-dichlorophenyl)-4-methyl-

1Hpyrazole-3-carboxamide hydrochloride (SR141716A) from Tocris (Bristol, UK). WIN55,212-2 and CP55,940 are potent synthetic cannabinoid agonists with similar affinity for CB_1 and CB_2 receptors. JZL184 is a potent, specific and irreversible inhibitor of monoacylglycerol lipase (MAGL) which increases the endogenous levels of 2-AG, an endocannabinoid with similar affinities for both cannabinoid receptors. SR141716A and SR144528 are specific antagonists of CB_1 and CB_2 receptors, respectively. Carbachol is a cholinergic agonist that activates muscarinic and nicotinic receptors.

WIN55,212-2 and JZL184 were administered intraperitoneally, once daily, in a volume of 5 ml/kg for seven consecutive days at the same time (between 8:00 and 9:00 am). Both cannabinoid compounds were dissolved in pure DMSO and diluted with Kolliphor EL (Sigma-Aldrich) and 0.9% saline to a final proportion of (1:1:18) respectively, as vehicle. Mice were randomly assigned to one of the following seven groups: (1) Non-Tg-vehicle (n = 10), (2) 3xTg-AD-vehicle (n = 10), (3) 3xTg-AD-WIN55,212-2 (0.1 mg/kg) (n = 10), (4) 3xTg-AD-WIN55,212-2 (1 mg/kg) (n = 10) , (5) 3xTg-AD-JZL184 (8 mg/kg) (n = 10), (6) Non-Tg-WIN55,212-2 (1 mg/kg) (n = 4) and (7) Non-Tg-JZL184 (8 mg/kg) (n = 4) (Figure 1).

Behavioral test

On the two days following the last dose, the behavioral effects of cannabinoid administration in the step-through passive avoidance were studied (PanLab, passive avoidance box LE872). During the acquisition session, the animals were placed in the open and illuminated compartment with heads facing the door, and then allowed to explore for 30 s. Then, the door was opened, allowing the mice to enter the dark compartment. The acquisition latency, with a cut-off time of 60 s, was recorded. When the animals crossed the door, it was closed and a foot-shock (0.4 mA/2 s) was delivered. Twenty-four hours later, during the retention session, the animals were placed again into the illuminated chamber and allowed to explore for 30 s. Then, the

door was opened and the step-through latency before entering the dark chamber, with a maximum cut-off time of 300 s, was recorded. No foot-shock was delivered in the retention session. Both sessions started at the same time (8:00 a.m.).

Tissue preparation

For immunohistochemical studies, 3 mice from groups 1 to 5 (see the section of "Drugs and treatments") were anesthetized with ketamine:xylazine (90:10 mg/kg), and transcardially perfused via the ascending aorta with 50 ml warm (37ºC), calcium-free Tyrode's solution (0.15 M NaCl, 5 mM KCl, 1.5 mM $MgCl_2$, 1 mM $MgSO_4$, 1.5 mM NaH_2PO_4, 5.5 mM Glucose, 25 mM $NaHCO_3$; pH 7.4), 0.5% heparinized, followed by 4% paraformaldehyde and 3% picric acid in 0.1M PB (4ºC) (100 ml/100 g b.w.). Brains were removed, post-fixed for 90 min at 4ºC, and cryoprotected in 20% phosphate buffer-sucrose solution overnight. The tissue was immersed in isopentane (-80ºC). In order to get an appropriate penetration of the antibodies and acceptable signal to noise ratio, 10 µm coronal sections were cryostat cut, mounted onto gelatin-coated slides, and stored at -25ºC.

For radioligand binding experiments, the remaining brain samples from groups 1 to 5 (n = 7 mice per group) and those from $CB_1^{-/-}$ (n = 2) and $CB_1^{+/+}$ (n = 2) mice (including spleen samples) were removed, fresh frozen to preserve the receptor functionality, and cut into 20 µm sections because the [^{3}H] and [^{14}C] microscales are calibrated for this thickness. Then, the sections were mounted onto gelatin-coated slides and stored at -25ºC.

Fixed and fresh frozen brain sections were obtained from five different stereotaxic coordinates in the coronal plane according to Paxinos and Watson (2001) [24]: Bregma 4.28 mm; Bregma 0.86 mm; Bregma -0.82 mm; Bregma -2.06 mm; Bregma -3.28.

Radioligands and chemical reagents

[^{35}S]GTPγS (1250 Ci/mmol) and [^{3}H]CP55,940 (131.8 Ci/mmol) were purchased from PerkinElmer (Boston MA, USA). The [^{14}C] and [^{3}H]-microscales used as standards were purchased from American Radiolabelled Chemicals (Saint Louis, MO, USA). The β-radiation sensitive films were purchased from Carestream. Bovine Serum Albumine (BSA), DL-dithiothreitol (DTT), adenosine deaminase (ADD), guanosine-5´-diphosphate (GDP), and guanosine-5´-O-3-thiotriphosphate (GTPγS) were acquired from Sigma-Aldrich. Finally, all the compounds necessary for the preparation of the different buffers were of the highest quality commercially available.

Cannabinoid receptor autoradiography

Two additional new consecutively cut sections from 3xTg-AD and Non-Tg mice (n = 7 mice per group) and from $CB_1^{-/-}$ and $CB_1^{+/+}$ mice (including brain and spleen) were dried and submerged in 50 mM Tris-HCl buffer containing 1% of BSA (pH 7.4) for 30 min at room temperature, followed by incubation in the same buffer in the presence of the CB_1/CB_2 radioligand, [^{3}H]CP55,940 (3 nM) for 2 h at 37ºC. Nonspecific binding was measured by competition with non-labelled CP55,940 (10 μM) in another consecutive slice. The CB_1 receptor antagonist, SR141716A (0.1 μM) and the CB_2 receptor antagonist, SR144528 (0.1 μ M), were used together with [^{3}H]CP55,940 in two consecutive slices to check the CB_1 or CB_2 receptor binding specificity. Then, sections were washed in ice-cold (4ºC) 50 mM Tris-HCl buffer supplemented with 1% BSA (pH 7.4) to stop the binding, followed by dipping in distilled ice-cold water and drying (4ºC). Autoradiograms were generated by exposure of the tissues for 21 days at 4ºC to β-radiation sensitive film together with [^{3}H]microscales used to specifically calibrate the optical densities to fmol/mg tissue equivalent (fmol/mg t.e.).

Labeling of activated $G_{i/o}$ proteins by [^{35}S]GTPγS binding assay

Additional newly cut consecutive sections (n = 7 mice per group) were dried, followed by two consecutive incubations in HEPES-based buffer (50 mM HEPES, 100 mM NaCl, 3 mM $MgCl_2$, 0.2 mM EGTA and 0.5% BSA, pH 7.4) for 30 min at 30ºC. Briefly, sections were incubated for 2 h at 30ºC in the same buffer supplemented with 2 mM GDP, 1 mM DTT, ADD (3 Units/l), and 0.04 nM [^{35}S]GTPγS. The [^{35}S]GTPγS basal binding was determined in two consecutive sections in the absence of agonist. The agonist-stimulated binding was determined in another consecutive section in the same reaction buffer in the presence of the CB_1/CB_2 receptor agonist, WIN55,212-2 (10 µM). Nonspecific binding was defined by competition with GTPγS (10 µM) in another section. Then, sections were washed twice in cold (4ºC) 50 mM HEPES buffer (pH 7.4), dried, and exposed to β-radiation sensitive film with a set of [^{14}C] standards to specifically calibrate the optical densities to nCi/g tissue equivalent (nCi/g t.e.).

A similar procedure was followed for mAChR in the presence of the cholinergic agonist carbachol (100 µM) (4 newly cut consecutive brain sections).

After 48 h, the films were developed, scanned, and quantified by transforming optical densities into nCi/g tissue equivalence units using a calibration curve defined by the known values of the [^{14}C] standards (NIH-IMAGE, Bethesda, MD, USA). Nonspecific binding values were subtracted from both agonist-stimulated and basal-stimulated conditions. The percentages of agonist-evoked stimulation were calculated from both the net basal and net agonist-stimulated [^{35}S]GTPγS binding densities according to the following formula: ([^{35}S]GTPγS agonist-stimulated binding x 100/[^{35}S]GTPγS basal binding)-100.

Immunofluorescence

Fixed 10 µm coronal sections from Non-Tg and 3xTg-AD mice were air dried for 20 min and washed by immersion in PBS for 15 min at room temperature. Then, the sections

were blocked with 5% normal goat serum in PBS buffer for 2 h at room temperature before being incubated with the primary antibody overnight at 4ºC.

To label CB_1 receptors, the primary rabbit antiserum against the CB_1 receptor, PA1-743, (Affinity BioReagents, CO, USA) was diluted [1:500] in TBS (0.1 M Tris, 0.15 M NaCl, pH 7.4) containing 0.5% milk powder. The tyramide signal amplification method was used to amplify the signal associated with the CB_1 receptor antiserum. Briefly, sections were washed for 30 min in TNT buffer (0.05% Tween 20 in TBS, pH 7.4) and blocked in TNB solution (10 ml TNT buffer, 0.05 g blocking reagent, DuPont) for 1 h at room temperature. Later, the sections were incubated with horseradish peroxidase-conjugated goat anti-rabbit secondary antibody (Perkin Elmer, MA, USA) for 1 h followed by tyramide fluorescein-based amplification (Perkin Elmer, MA, USA) process in complete darkness for 10 min at room temperature. Sections were extensively rinsed in TBS.

To label the subtype-2 muscarinic receptor (M_2 mAChR), rabbit anti-M_2 mAChR (EMD Millipore, CA, USA) was diluted in PBS (0.1 M, pH 7.4) to a final concentration of 1:400. Then, the primary antibody was revealed by incubation (30 min at 30ºC) with donkey anti-rabbit CY3. To study the cellular localization of CB_1 receptor and M_2 mAChR on glutamatergic or GABAergic neurons, tissue slices were incubated with primary guinea pig anti-vesicular glutamate transporter 3 (VGLUT3) and mouse anti-glutamic acid decarboxylase isoform 65kDa (GAD65) (EMD Millipore, CA, USA) diluted in PBS (0.1 M, pH 7.4) to a final concentration of 1:750 in both cases, and revealed by incubation (30 min at 30ºC) with secondary Alexa488 or Alexa555 [1:250] donkey anti-guinea pig and FITC [1:80] or Alexa 555 donkey anti-mouse. Then, sections were incubated with Hoechst [$1:10^6$] for 15 min, washed, and mounted with p-phenylendiamine-glycerol.

Sections were screened with an Axioskop microscope (Zeiss). 630-fold magnification images for colocalization were acquired on an Axioskop Observer A1 inverted

microscope (Zeiss) by optical sectioning (0.24 µm/X-Y-Z-resolution) using structured illumination (ApoTome-Zeiss). Images were created with ZEN2014 software (Zeiss) and defined as signal being present without physical separation.

Statistical analysis

A two-tailed unpaired Student's *t*-test was used to determine differences between genotypes (Non-Tg *versus* 3xTg-AD; groups 1 and 2) and one-way analysis of variance (ANOVA) for comparisons between all the groups of mice including the vehicle-treated Non-Tg group (1 to 5), followed by Bonferroni´s *post hoc* test. The step-through latencies were represented as Kaplan-Meier survival curves, and for comparisons the nonparametric Log-rank/Mantel-Cox test was used which is appropriate when censored data must be analyzed, as explained in [25]. The existence of animals that reached the cut-off time of 300 s was the reason to choose this rigorous statistical analysis. Behavioral correlations with neurochemical data were analyzed with Pearson's correlation. Statistical significance was set at $p < 0.05$.

Results

Behavioral impairment in 3xTg-AD mice is restored following the subchronic cannabinoid administration

3xTg-AD and Non-Tg mice differed in acquisition and retention latencies during the passive avoidance test. 3xTg-AD mice took significantly longer to enter the dark compartment than Non-Tg mice ($p = 0.0002$, Student's *t*-test; $p < 0.01$, one-way ANOVA followed by Bonferroni´s *post hoc* test for multiple comparisons) (Figure 2A). Moreover, 40% failed to remember the foot-shock as compared to the positive response shown in 100% of Non-Tg mice ($p = 0.029$, Log-Rank/Mantel-Cox test) (Figure 2B).

No differences in the passive avoidance test were observed in Non-Tg mice, following the subchronic administration of the full agonist WIN55,212-2 (1 mg/kg). A similar effect was observed by the subchronic treatment with JZL184 (8 mg/kg), a potent inhibitor of monoacylglycerol lipase (MAGL) that increases the 2-AG endogenous levels (Supplementary Figure). However, the cannabinoid treatments in 3xTg-AD mice reduced the increase in acquisition latencies observed in the vehicle-treated 3xTg-AD group (one-way ANOVA followed by Bonferroni´s *post hoc* test for multiple comparisons), restoring the latencies to Non-Tg levels (Figure 2C). Thus, WIN55,212-2 elicited a behavioral dose-response with slight (0.1 mg/kg, reduction 35%) or marked (1 mg/kg, reduction 50%, $p < 0.05$) reductions in acquisition latency as compared with those observed in the vehicle-treated 3xTg-AD animals. JZL184 (8 mg/kg), a MAGL inhibitor, induced a similar effect (reduction 42%, $p < 0.05$) (Figure 2C). The treatments elicited subtle variations in memory (step-through latency) in 3xTg-AD mice, as shown in the Kaplan-Meier representation, although they did not reach statistical significance (Figure 2D).

Endocannabinoid signaling in 3xTg-AD is restored following CB_1 receptor desensitization

[^{3}H]CP55,940 radioligand, that shows a similar affinity for CB_1 and CB_2 receptors, was used to analyze the cannabinoid receptor density. Quantitative densitometry showed increased density of cannabinoid receptors (specific [^{3}H]CP55,940 binding sites) in the BLA ($p = 0.0008$, Student´s *t*-test; $p < 0.001$, one-way ANOVA followed by Bonferroni´s *post hoc* test for multiple comparisons) and the lateral olfactory tract nucleus ($p = 0.0274$, Student´s *t*-test; $p < 0.05$, one-way ANOVA followed by Bonferroni´s *post hoc* test for multiple comparisons), but a decrease in the glomerular olfactory bulb ($p < 0.0001$, Student's *t*-test; $p < 0.001$, one-way ANOVA followed by Bonferroni´s *post hoc* test for multiple comparisons) of vehicle-treated 3xTg-AD mice (Figures 2E and 5A)

(Tables 1 and supplementary Table 1). [^{3}H]CP55,940 autoradiography further revealed specific modifications in cerebral cannabinoid receptor density following the subchronic eCB system activation. The low dose of WIN55,212-2 (0.1 mg/kg) did not modify cannabinoid receptor density, but a higher dose of WIN55,212-2 (1 mg/kg) induced a significant decrease in BLA (22%; $p < 0.05$) which shows a dose-dependent effect in eCB signaling. Furthermore, the administration of JZL184 dramatically reduced the cannabinoid receptor density, including cortical ($p < 0.01$), hippocampal ($p < 0.001$), and amygdaloid regions ($p < 0.001$) (one-way ANOVA followed by Bonferroni´s *post hoc* test for multiple comparisons) (Figures 2E and 5B) (Table 1 and supplementary Table 1).

To determine the specific subtype of the cannabinoid receptor involved in the observed changes, SR141716A and SR144528, well-known selective antagonists for CB_1 and CB_2 receptors respectively, were used in combination with brain and spleen samples from $CB_1^{+/+}$ and $CB_1^{-/-}$ mice. SR141716A blocked [^{3}H]CP55,940 binding in brain slices from 3xTg-AD and $CB_1^{+/+}$ mice, but failed in spleen, as was expected in a tissue that exclusively expresses the CB_2 receptor subtype. SR144528 completely blocked [^{3}H]CP55,940 binding in spleen slices but failed in brain samples. $CB_1^{-/-}$ mice showed an almost complete absence of [^{3}H]CP55,940 binding in the brain, whereas they displayed similar binding levels in the spleen to those obtained in $CB_1^{+/+}$ mice, which demonstrates the selectivity of both antagonists and the specific deregulation of the CB_1 subtype in 3xTg-AD mice (Figure 3). The contribution of each cannabinoid receptor subtype to the observed changes was demonstrated by measuring [^{3}H]CP55,940 binding in the presence of SR141716A, which specifically blocks the radioligand binding to CB_1 receptors or, in the presence of SR144528, which specifically blocks the radioligand binding to CB_2 receptors. Almost all the binding in the brain of 3xTg-AD mice and Non-Tg was blocked in the presence of SR141716A (i.e., the optical density was comparable to non-specific binding values). On the other hand,

the optical density in the presence of SR144528 was comparable to that obtained in the total binding, i.e., in the absence of any antagonist. (Data not shown). These results demonstrate both the absence of detectable changes in CB_2 receptor density in seven-month-old male 3xTg-AD mice and the CB_1 receptor-mediated effects on the behavioral outcomes.

Functional coupling of CB_1 receptors in 3xTg-AD mice

[^{35}S]GTPγS autoradiography allows anatomical localizing and quantification of receptor-dependent $G_{i/o}$ protein activity directly in tissue. Basal activity was similar in the two genotypes. The activity of CB_1 receptors evoked by WIN55,212-2 (10 μM), was higher in the BLA of 3xTg-AD ($p = 0.0303$, Student´s *t*-test; $p < 0.05$, one-way ANOVA followed by Bonferroni´s *post hoc* test for multiple comparisons) (Figure 4B and 5E) but lower in several areas such as the striatum ($p = 0.0285$, Student´s *t*-test; $p < 0.05$, one-way ANOVA followed by Bonferroni´s *post hoc* test for multiple comparisons), the glomerular olfactory bulb ($p = 0.0043$, Student´s *t*-test; $p < 0.01$, one-way ANOVA followed by Bonferroni´s *post hoc* test for multiple comparisons), and the molecular layer of hippocampal dentate gyrus ($p = 0.0040$, Student's *t*-test; $p < 0.05$, one-way ANOVA followed by Bonferroni´s *post hoc* test for multiple comparisons) (Table 2 and supplementary Table 2).

Functional [^{35}S]GTPγS autoradiography of CB_1 receptor activation showed a non-significant decrease of 24% and 32% in the BLA following treatment with WIN55,212-2 (1 mg/kg) and JZL184 (8 mg/kg), respectively (Figures 4C-D and 5F) (Table 2 and supplementary Table 2). The basal binding of [^{35}S]GTPγS was not modified by the different cannabinoid compounds, which probably indicates the absence of changes in the constitutive activity of G protein-coupled receptors (GPCR). (Data analyzed with a one-way ANOVA followed by Bonferroni´s *post hoc* test for multiple comparisons).

Regression analyses

The regression analyses showed that 50% and 33% of the variation in the acquisition latencies recorded in 3xTg-AD mice were related to changes in CB_1 receptor density ([^{3}HCP55,940 binding) in the BLA (r^2 = 0.5096, p = 0.0091) and/or to changes in CB_1 receptor activity (evoked by WIN55,212-2) (r^2 = 0.3299, p = 0.0508), respectively (Figure 5C, G). No statistically significant correlations were found when other brain areas were compared such as the lateral olfactory tract nucleus and glomerular olfactory bulb (p = ns). Both treatments, JZL184 (8 mg/kg) and WIN55,212-2 (1 mg/kg), decreased the acquisition latencies of 3xTg-AD mice to Non-Tg mice control values due to the pharmacological desensitization of CB_1 receptors to levels even lower than those observed in Non-Tg mice. When the groups were compared all together, a positive and statistically significant correlation between CB_1 receptor density in the BLA and acquisition latencies was found, showing that 25% of the acquisition latency variation may be explained by changes in CB_1 receptor density (r^2 = 0.2499, p = 0.013), but not by changes in CB_1 receptor activity (Figure 5D, H).

Decreased M_2/M_4 mAChR-mediated activity in 3xTg-AD is modulated by cannabinoid administration

We analyzed the functional coupling of mAChR to $G_{i/o}$ proteins evoked by carbachol (100 μM) in both genotypes and in cannabinoid-based treated 3xTg-AD mice. Transgenic mice showed decreased functional coupling in the BLA (p = 0.0258, Student´s *t*-test; p < 0.05 one-way ANOVA followed by Bonferroni´s *post hoc* test for multiple comparisons), in the lateral amygdala (p = 0.0303, Student´s *t*-test; p < 0.05 one-way ANOVA followed by Bonferroni´s *post hoc* test for multiple comparisons) and hippocampal pyramidal CA1 (p = 0.0227, Student´s *t*-test; p < 0.05 one-way ANOVA followed by Bonferroni´s *post hoc* test for multiple comparisons). Moreover, increased M_2/M_4 mAChR receptor activity was found in the glomerular olfactory bulb (p = 0.0095

Student´s *t*-test; $p < 0.01$ one-way ANOVA followed by Bonferroni´s *post hoc* test for multiple comparisons) of 3xTg-AD mice (Figure 4F and Table 3). The administration of 1 mg/kg of WIN55,212-2 was able to increase the M_2/M_4 mAChR-mediated activity to similar values of Non-Tg mice; up to 60% in the BLA ($p < 0.05$ *vs* 3xTg-AD vehicle, one-way ANOVA followed by Bonferroni´s *post hoc* test for multiple comparisons) and up to 100% in the lateral amygdala ($p < 0.01$ *vs* 3xTg-AD-vehicle one-way ANOVA followed by Bonferroni´s *post hoc* test for multiple comparisons) (Figure 4G). No modulation of M_2/M_4 mAChR-mediated activity was observed in other brain areas (Table 3 and supplementary Table 3).

CB_1 receptors in BLA and M_2 mAChR in hippocampus colocalize with GABAergic terminals in 3xTg-AD mice

To further understand the physiological cellular mechanisms of the observed changes in cannabinoid and muscarinic signaling, the immunofluorescence studies were carried out in BLA and in the ventral hippocampus (Bregma -2.06 mm; Bregma -3.28 respectively, according to Paxinos and Watson (2001)). The different nuclei of the amygdala exhibited distinct CB_1 receptor immunostaining patterns and were clearly defined. The dense CB_1 receptor immunoreactive *puncta* observed at the BLA suggested a presynaptic localization of CB_1 receptor. Immunofluorescence assays for VGLUT3 and GAD65 and the subsequent colocalization studies suggested the inhibitory nature of CB_1 receptor containing presynaptic boutons (Figure 6).

M_2 mAChR immunoreactivity was differentially localized along the hippocampal formation. The pyramidal neurons of CA1-CA3 displayed a dense network of fibers delineating the perikarya in basket-like formations. VGLUT3 displayed a somato-dendritic immunostaining, but GAD65 immunoreactivity was present as a dense plexus of fibers around pyramidal neurons with a similar distribution to M_2 mAChR. Colocalization studies confirmed the presence of M_2 mAChR in presynaptic GABAergic

terminals with a high degree of co-immunolabeling with GAD65, but an almost total absence of expression on VGLUT3 positive cells (Figure 7). However, in the amygdala, the M_2 mAChR are not distributed neither in presynaptic GABAergic terminals nor in VGLUT3 positive compartments (images not shown).

Discussion

The eCB system has emerged as a promising target for the treatment of several neurodegenerative disorders including AD. Here, we provide evidence of neuroanatomical and neurochemical modifications related to the eCB neuromodulatory system and muscarinic cholinergic signaling in the 3xTg-AD mice model and their behavioral outputs at 7 months of age, once the cognitive impairment is clearly established and is concurrent with limbic system-mediated symptoms [17]. The results point to the eCB system as a key modulator of neuronal homeostasis involved in learning or acquisition processes.

The present study examines, for the first time, the neurochemical effects of cannabinoid agonism in 3xTg-AD mice and their behavioral correlates in a learning and memory task under fear conditions, which can be relevant in relation to clinical interventions at the onset of disease.

CB_1 receptor desensitization in BLA and decrease of acquisition latency in 3xTg-AD mice to Non-Tg levels

The results provide evidence that repeated cannabinoid administration was able to decrease the acquisition latency in 3xTg-AD mice to Non-Tg levels, which is related to the CB_1 receptor desensitization recorded in the BLA. Interestingly, we observed both, a down-regulation of CB_1 receptors and an attenuation of their functional coupling to $G_{i/o}$ proteins induced by the subchronic administration of JZL184, comparable to the

results obtained in a previous study but at different doses [26]. Moreover, the administration of WIN55,212-2 (1 mg/kg) decreases the acquisition latency and slightly also the CB_1 receptor functionality in the BLA.

Our results confirm previous findings reported for JZL184, which selectively increased brain 2-AG and pointed to the inhibition of the MAGL as a promising target to indirectly potentiate the activation of CB_1 receptors [9, 27]. In this sense, pharmacological blockade or genetic deletion of MAGL dramatically raises brain 2-AG levels, down-regulates CB_1 receptors, and modulates synaptic plasticity, learning, memory and anxiety-like behavior [28]. A recent study shows that the intra-BLA administration of both AEA and 2-AG hydrolysis inhibitors is able to attenuate anxiety-like responses, which are dependent on deregulated levels of eCB in the amygdala [29]. Conversely, chronic CB_1 receptor blockade induced an up-regulation of CB_1 receptor expression and modified anxiety-like behaviors [30]. The contribution of the eCB levels or the observed CB_1 receptor signaling regulation in the BLA of 3xTg-AD mice, to the reported differences in learning or acquisition latencies, should be clarified in further studies.

The results of the passive avoidance test, used to evaluate learning and memory of an aversive electrical stimulus under stressful conditions, could indicate fear and/or diminished motivation to explore as shown in a lesioned rat model of AD [31]. 3xTg-AD mice displayed higher acquisition latencies as compared to controls. Fear or anxiety-like responses have been shown in the contextual fear-conditioning, in the open field, dark-light box and in the passive avoidance tests in this mouse model of AD at 6 months of age [18, 19, 21]. Stover et al. [32] observed that 6-month-old 3xTg-AD mice showed enhanced motor performance on the rotarod, but there was no difference in voluntary motor activity between genotypes. We observed that the subchronic administration of cannabinoids to Non-Tg mice did not modify the behavior in the passive avoidance test, suggesting that the treatments do not cause changes in voluntary movement. A specific battery of motor behavior test in 3xTg-AD mice treated

with cannabinoids at different ages is necessary since their effects depend on the used test, the age and rodent strain [9, 33].

Regarding the possible involvement of cannabinoid signaling in these behavior modulations, we report specific changes in density and activity of CB_1 receptors, indicative that cannabinoid signaling is potentiated in the BLA and attenuated in the olfactory bulb and hippocampal dentate gyrus of transgenic mice. Our results support the studies which report a significant increase in CB_1 receptor density in the BLA when only intracellular Aβ accumulation can be detected and may be related to the symptoms of fear shown by these mice [15, 21]. The specificity for CB_1 receptor was demonstrated by the anatomical pattern of distribution of [^{3}H]CP55,940 binding sites in brain compared to that of spleen. Therefore, tangentially to the objective of this work, an absence of significant CB_2 receptor-mediated detectable signal in the CNS of seven-month-old 3xTg-AD mice was found. Although, up-regulation of CB_2 receptors has been previously associated to neuroinflammation in AD patients, these results show the lack of oligomeric-Aβ-associated neuroinflammatory response related to CB_2 receptor signaling, coinciding with the onset of earlier markers of disease in 3xTg-AD mice [34-37].

Depending on the specific location of CB_1 receptors, on inhibitory or excitatory neurons, the functional and physiological outcomes of deregulated endocannabinoid signaling may be useful to understand the present results. Previous studies had reported that stressing factors result in a modulation of the endocannabinoid levels in the amygdala, and also induce a subsequent CB_1 receptor-mediated suppression of GABA release specifically in the BLA [34, 38-40]. The immunochemical results in the BLA showed that the localization of CB_1 receptors is more frequent in GABAergic than in glutamatergic compartments, even though CB_1 receptors have been previously detected in both of them [41-43]. The detected CB_1 receptors in BLA were in the proximity of GAD65 (the enzyme glutamate decarboxylase; GAD, associated with inhibitory nerve termini) [44].

In addition, the detection of VGLUT3 was used to identify both excitatory presynaptic boutons and glutamatergic somatodendritic compartments [45, 46]. Although CB_1 receptors are present in both GABAergic and glutamatergic cellular compartments in areas such as the hippocampus, their activity seems to be lower in the inhibitory terminals [47]. However, in BLA, CB_1 receptors are highly expressed in axon terminals of GABAergic neurons modulating GABA release via a presynaptic mechanism [48]. Some authors have related long-lasting increase of anxiety-like behaviors with a hyperactivity of BLA as consequence of a decrease in the inhibitory synaptic transmission [49-50]. Thus, eCB-mediated suppression of inhibitory inputs to BLA neurons is involved in the cellular mechanism for the stress-induced increases in anxiety-like behavior [51]. Different studies suggest that drugs targeting the endocannabinoid system (e.g. endocannabinoid degrading enzymes inhibitors) could be used as a potential treatment strategy for anxiety and mood disorders [38-39, 51-53]. Globally, the present findings suggest an up-regulation of the eCB tone in 3xTg-AD mice in areas such as the BLA, which should alter the local excitatory–inhibitory balance, as a possible underlying mechanism that may be involved in the observed differences in the acquisition phase of the test. Furthermore, a reversion of the acquisition latencies to those of Non-Tg mice was recorded after the eCB signaling attenuation mediated by a pharmacological desensitization of CB_1 receptors, suggesting that suppression of inhibition induced by increase of CB_1 signaling in the BLA of 3xTg-AD mice, would result in an enhanced excitatory input.

This decrease in GABAergic neurotransmission would act as an important component of the neurobiological mechanisms controlling fear-related behavioral responses probably contributing to the observed differences in acquisition latency, which should be further confirmed using additional behavioral studies.

Moreover, the administration of WIN55,212-2 (1 mg/kg), but not JZL184, was able to induce a significant increase in the activity mediated by mAChR in the latero-BLA

complex and hippocampus but not in the cortex or in the glomerular olfactory bulb. This possible crosstalk between both systems in limbic areas, suggests a selective effect dependent on the cannabinoid treatment and on the brain region. This specific CB_1 receptor-driven modulation of cholinergic neurotransmission in the amygdala could also be involved in the behavioral outcomes recorded with the passive avoidance test. In addition, the results support previous studies describing the role of BLA cholinergic system, via mAChR, in memory retrieval in fear-induced learning [54-55].

On the other hand, M_2 mAChR, which are not localized in CB_1-GABAergic terminals, could be responsible of the crosstalk between both systems in latero-BLA. Further anatomical and behavioral studies are necessary to understand the meaning of CB_1 receptor-induced modulation of the muscarinic control on acquisition latency, as a possible indicator of states involving fear, attention, agitation or confusion.

The subchronic administration of WIN55,212-2 or JZL184 failed to induce significant modifications in step-through latency in either Non-Tg or 3xTg-AD mice

Regarding the memory process, step-through latency clearly distinguished the cognitively impaired AD-phenotype of 3xTg-AD mice, in accordance to previous studies [19, 56]. However, under the present experimental conditions, we cannot rule out the possibility that the differences found in the acquisition, or even in the consolidation, may also contribute to the performance of step-through latency. The desensitization of CB_1 receptors by means of subchronic administration ofWIN55,212-2 or JZL184 failed to induce significant modifications in step-through latency in either Non-Tg or 3xTg-AD mice. However, previous studies analyzing the effects of other CB_1 agonists in a different transgenic mice model of AD have reported a reduction in cognitive impairment [57].

On the other hand, the analgesic effects of acute CB_1 receptor activation are well known [58], and one may speculate that the administration of cannabinoids may contribute to alter the pain perception leading to increase the pain threshold of the foot-shock [59]. In this sense, the repeated administration of both high (40 mg/kg) or low (8 mg/kg) doses of JZL184, the latter being that used in the present study, were able to induce a loss of the CB_1 receptor-mediated analgesic activity, probably as a consequence of the CB_1 receptor down-regulation [9, 60-61]. This has been extensively reviewed in a recent paper [62]. Therefore, the subtle variations in step-through latencies recorded after the cannabinoid administration should not be biased by a possible increase in analgesia. Moreover, the limbic system involving the cholinergic neurotransmission may be controlling specifically the consolidation and extinction of aversive or traumatic memories [63]. Further behavioral analyses by means of non-aversive stimulus-based learning and memory tests will contribute to clarify this issue since 3xTg-AD mice do not seem to differ from Non-Tg in pain thresholds [19, 64]. Interestingly, muscarinic activation, through the M_2 mAChR subtype, modulates hippocampal neuronal plasticity, and the lack of these receptors leads to cognitive impairment in the passive avoidance test [65-66]. The present immunofluorescence studies revealed the presynaptic localization of M_2 mAChR in GABAergic terminals, presumably making contact with postsynaptic VGLUT3 immunoreactive pyramidal neurons in CA1-CA3. These results are consistent with those reported in rat brain, suggesting that ACh via M_2 mAChR reduces GABA release from presynaptic inhibitory terminals. The final effect could be an increase of the activity in the dendritic region of pyramidal neurons, as previously described [67-68]. The significant reduction in choline acetyltransferase activity described in the hippocampus from middle-aged 3xTg-AD mice, not associated with the loss of cholinergic neurons, may be related to the observed decrease in mAChR functionality leading to enhance the inhibitory tone of the pyramidal neurons from CA1 [13]. We

suggest that intraneuronal accumulation of Aβ, beginning at 4 months of age, may trigger an early deregulation of the hippocampal muscarinic neurotransmission, as observed in seven-month-old 3xTg-AD mice, thereby contributing to the cognitive impairment observed in this model [17]. Moreover, an excitatory/inhibitory imbalance mediated by a deregulated presynaptic muscarinic neurotransmission in the hippocampus may underlie the impaired synaptic plasticity, i.e., the neurobiological substrate for creating and maintaining new memories.

Conclusions

We provide evidence that both endocannabinoid and muscarinic signaling are altered in seven-month-old male 3xTg-AD mice, when earlier pathological markers of disease are clearly established. CB_1 receptor-mediated hyperactivity in BLA may have behavioral correlates that correspond with the restoration to control levels after pharmacological desensitization of CB_1 receptors.

WIN55,212-2 administration restores muscarinic neurotransmission in vulnerable limbic areas to Non-Tg levels demonstrating a crosstalk between both systems.

CB_1 receptor desensitization could be a plausible strategy to palliate specific behavior impairments associated with genetic variants of AD.

Acknowledgements

This work was supported by the Departments of Economic Development (Elkartek KK-2016/00045) and Education (IT975-16) of the Basque Government. Technical and human support provided by General Research Services SGIker from University of the Basque Country (UPV/EHU), co-financed by Ministry of Economy and Competitiveness (MINECO) of the Spanish Government, European Regional Development Fund (ERDF), and European Social Fund (ESF). Dr. Frank M LaFerla, University of California Irvine, Irvine, CA, (USA) for kindly providing the progenitors of the Spanish colonies of 3xTg-AD and non-transgenic mice. A. LL. is the recipient of a fellowship from the Basque Government (BFI 2012-119). All authors have seen and approved the manuscript being submitted. The authors declare no conflict of interest.

References

[1] Cummings JL, Back C (1998) The cholinergic hypothesis of neuropsychiatric symptoms in Alzheimer's disease. *Am J Geriatr Psychiatry* **6**(2 Suppl 1), S64-78.

[2] Cummings J, Lai TJ, Hemrungrojn S, Mohandas E, Yun Kim S, Nair G, Dash A (2016) Role of Donepezil in the Management of Neuropsychiatric Symptoms in Alzheimer's Disease and Dementia with Lewy Bodies. *CNS Neurosci Ther* **22**, 159-166.

[3] Davies P, Maloney AJ (1976) Selective loss of central cholinergic neurons in Alzheimer's disease. *Lancet* **2**, 1403.

[4] Perry EK, Tomlinson BE, Blessed G, Bergmann K, Gibson PH, Perry RH (1978) Correlation of cholinergic abnormalities with senile plaques and mental test scores in senile dementia. *Br Med J* **2**, 1457-1459.

[5] Bartus RT, Dean RL, Beer B, Lippa AS (1982) The cholinergic hypothesis of geriatric memory dysfunction. *Science* **217**, 408-414.

[6] Whitehouse PJ, Price DL, Struble RG, Clark AW, Coyle JT, Delon MR (1982) Alzheimer's disease and senile dementia: loss of neurons in the basal forebrain. *Science* **215**, 1237-1239.

[7] Rodríguez-Puertas R, Pazos A, Zarranz JJ, Pascual J (1994) Selective cortical decrease of high-affinity choline uptake carrier in Alzheimer's disease: an autoradiographic study using 3H-hemicholinium-3. *J Neural Transm Park Dis Dement Sect* **8**, 161-169.

[8] Rodríguez-Puertas R, Pascual J, Vilaró T, Pazos A. (1997) Autoradiographic distribution of M1, M2, M3, and M4 muscarinic receptor subtypes in Alzheimer's disease. *Synapse* **26**, 341-350.

[9] Busquets-Garcia A, Puighermanal E, Pastor A, de la Torre R, Maldonado R, Ozaita A (2011) Differential role of anandamide and 2-arachidonoylglycerol in memory and anxiety-like responses. *Biol Psychiatry* **70**, 479-486.

[10] Westlake TM, Howlett AC, Bonner TI, Matsuda LA, Herkenham M (1994) Cannabinoid receptor binding and messenger RNA expression in human brain: an in vitro receptor autoradiography and in situ hybridization histochemistry study of normal aged and Alzheimer's brains. *Neuroscience* **63**, 637-652.

[11] Manuel I, González de San Román E, Giralt MT, Ferrer I, Rodríguez-Puertas R (2014). Type-1 cannabinoid receptor activity during Alzheimer's disease progression. *J Alzheimers Dis* **42**, 761-766.

[12] Bedse G, Romano A, Lavecchia AM, Cassano T, Gaetani S (2015) The role of endocannabinoid signaling in the molecular mechanisms of neurodegeneration in Alzheimer's disease. *J Alzheimers Dis* **43**, 1115-1136.

[13] Perez SE, He B, Muhammad N, Oh KJ, Fahnestock M, Ikonomovic MD, Mufson EJ (2011) Cholinotrophic basal forebrain system alterations in 3xTg-AD transgenic mice. Neurobiol Dis. **41**, 338-352.

[14] Manuel I, Lombardero L, LaFerla FM, Giménez-Llort L, Rodríguez-Puertas R, (2016) Activity of muscarinic, galanin and cannabinoid receptors in the prodromal and advanced stages in the triple transgenic mice model of Alzheimer's disease. *Neuroscience* **329**, 284-293.

[15] Bedse G, Romano A, Cianci S, Lavecchia AM, Lorenzo P, Elphick MR, Laferla FM, Vendemiale G, Grillo C, Altieri F, Cassano T, Gaetani S (2014) Altered expression of the CB1 cannabinoid receptor in the triple transgenic mouse model of Alzheimer's disease. *J Alzheimers Dis* **40**, 701-712.

[16] Oddo S, Caccamo A, Shepherd JD, Murphy MP, Golde TE, Kayed R, Metherate R, Mattson MP, Akbari Y, LaFerla FM (2003) Triple-transgenic model of Alzheimer's disease with plaques and tangles: intracellular Abeta and synaptic dysfunction. *Neuron* **39**, 409-421.

[17] Billings LM, Oddo S, Green KN, McGaugh JL, LaFerla FM (2005) Intraneuronal Abeta causes the onset of early Alzheimer's disease-related cognitive deficits in transgenic mice. *Neuron* **45**, 675-688.

[18] Giménez-Llort, L, Blázquez G, Cañete T, Johansson B, Oddo S, Tobeña A, LaFerla FM, Fernández-Teruel A (2007) Modeling behavioral and neuronal symptoms of Alzheimer's disease in mice: a role for intraneuronal amyloid. *Neurosci Biobehav Rev* **31**, 125-147.

[19] Filali M, Lalonde R, Theriault P, Julien C, Calon F, and Planel E (2012) Cognitive and non-cognitive behaviors in the triple transgenic mouse model of Alzheimer’s disease expressing mutated APP, PS1, and Mapt (3xTg-AD). *Behav Brain Res* **234**, 334–342.

[20] Nelson RL, Guo Z, Halagappa VM, Pearson M, Gray AJ, Matsuoka Y, Brown M, Martin B, Iyun T, Maudsley S, Clark RF, Mattson MP (2007) Prophylactic treatment with paroxetine ameliorates behavioral deficits and retards the development of amyloid and tau pathologies in 3xTgAD mice. *Exp Neurol* **205**, 166-176.

[21] España J, Giménez-Llort L, Valero J, Miñano A, Rábano A, Rodriguez-Alvarez J, LaFerla FM, Saura C (2010) Intraneuronal beta-amyloid accumulation in the amygdala enhances fear and anxiety in Alzheimer’s disease transgenic mice. *Biol Psychiatry* **67**, 513-521.

[22] Rasool S, Martinez-Coria H, Wu JW, LaFerla F, Glabe CG (2013) Systemic vaccination with anti-oligomeric monoclonal antibodies improves cognitive function by

reducing Aβ deposition and tau pathology in 3xTg-AD mice. *J Neurochem* **126**, 473-482.

[23] Pietropaolo S, Feldon J, Yee BK (2014). Environmental enrichment eliminates the anxiety phenotypes in a triple transgenic mouse model of Alzheimer's disease. *Cogn Affect Behav Neurosci* **14**, 996-1008.

[24] Paxinos G, Franklin BJ (2001). The mouse brain in stereotaxic coordinates. San Diego: Academic Press, 2nd Edition.

[25] Barreda-Gómez G, Lombardero L, Giralt MT, Manuel I, Rodríguez-Puertas R (2015) Effects of galanin subchronic treatment on memory and muscarinic receptors. *Neuroscience* **293**, 23-34.

[26] Kinsey SG, Wise LE, Ramesh D, Abdullah R, Selley DE, Cravatt BF, Lichtman AH (2013) Repeated low-dose administration of the monoacylglycerol lipase inhibitor JZL184 retains cannabinoid receptor type 1-mediated antinociceptive and gastroprotective effects. *J Pharmacol Exp Ther* **345**, 492-501.

[27] Kinsey SG, O'Neal ST, Long JZ, Cravatt BF, Lichtman AH (2011) Inhibition of endocannabinoid catabolic enzymes elicits anxiolytic-like effects in the marble burying assay. *Pharmacol Biochem Behav* **98**, 21-27.

[28] Pan B, Wang W, Blankman JL, Cravatt BF, Liu QS (2011) Alterations of endocannabinoid signaling, synaptic plasticity, learning, and memory in monoacylglycerol lipase knock-out mice. *J Neurosc* **31**, 13420-13430.

[29] Morena M, Leitl KD, Vecchiarelli,HA, Gray JM, Campolongo P, Hill MN (2016) Emotional arousal state influences the ability of amygdalar endocannabinoid signaling to modulate anxiety. Neuropharmacology 111, 59-69.

[30] Tambaro S, Tomasi ML, Bortolato M (2013) Long-term CB_1 receptor blockade enhances vulnerability to anxiogenic-like effects of cannabinoids. Neuropharmacology 70, 268-277.

[31] Babalola PA, Fitz NF, Gibbs RB, Flaherty PT, Li PK, Johnson DA (2012) The effect of the steroid sulfatase inhibitor (p-O-sulfamoyl)-tetradecanoyl tyramine (DU-14) on learning and memory in rats with selective lesion of septal-hippocampal cholinergic tract. *Neurobiol Learn Mem* **98**, 303-310.

[32] Stover KR, Campbell MA, Van Winssen CM, Brown RE (2015) Analysis of motor function in 6-month-old male and female 3xTg-AD mice. *Behav Brain Res* **281**, 16-23. [33] Pandolfo P, Pamplona FA, Prediger RD, Takahashi RN (2007) Increased sensitivity of adolescent spontaneously hypertensive rats, an animal model of attention deficit hyperactivity disorder, to the locomotor stimulation induced by the cannabinoid receptor agonist WIN 55,212-2. *Eur J Pharmacol* **563**, 141-148.

[34] Benito C, Núñez E, Tolón RM, Carrier EJ, Rábano A, Hillard CJ, Romero J (2003) Cannabinoid CB2 receptors and fatty acid amide hydrolase are selectively overexpressed in neuritic plaque-associated glia in Alzheimer's disease brains. *J Neurosci* **23**, 11136-11141.

[35] Tolón RM, Núñez E, Pazos MR, Benito C, Castillo AI, Martínez-Orgado JA, Romero J (2009) The activation of cannabinoid CB2 receptors stimulates in situ and in vitro beta-amyloid removal by human macrophages. *Brain Res* **1283**, 148-154.

[36] Schmöle AC, Lundt R, Ternes S, Albayram Ö, Ulas T, Schultze JL, Bano D, Nicotera P, Alferink J, Zimmer A (2015) Cannabinoid receptor 2 deficiency results in reduced neuroinflammation in an Alzheimer's disease mouse model. *Neurobiol Aging* **36**, 710-719.

[37] Aso E, Ferrer I (2016) CB2 Cannabinoid Receptor As Potential Target against Alzheimer's Disease. *Front Neurosci* **10**, 243.

[38] Jenniches I, Ternes S, Albayram O, Otte DM, Bach K, Bindila L, Michel K, Lutz B, Bilkei-Gorzo A, Zimmer A (2015) Anxiety, stress, and fear response in mice with reduced endocannabinoid levels. *Biol Psychiatry* **79**, 858-868.

[39] Di S, Itoga CA, Fisher MO, Solomonow J, Roltsch EA, Gilpin NW, Tasker JG, (2016) Acute Stress Suppresses Synaptic Inhibition and Increases Anxiety via Endocannabinoid Release in the Basolateral Amygdala. *J Neurosci* **36**, 8461-8470.

[40] Bedse G, Hartley ND, Neale E, Gaulden AD, Patrick TA, Kingsley PJ, Uddin MJ, Plath, N Marnett LJ, Patel S (2017) Functional Redundancy Between Canonical Endocannabinoid Signaling Systems in the Modulation of Anxiety. *Biol Psychiatry* **82**, 488-499.

[41] Kodirov SA, Jasiewicz J, Amirmahani P, Psyrakis D, Bonni K, Wehrmeister M, Lutz B (2009) Endogenous cannabinoids trigger the depolarization-induced suppression of excitation in the lateral amygdala. *Learn Mem* **17**, 43-49.

[42] Robinson SL, Alexander NJ, Bluett RJ, Patel S, McCool BA (2016) Acute and chronic ethanol exposure differentially regulate CB1 receptor function at glutamatergic synapses in the rat basolateral amygdala. *Neuropharmacology* **108**, 474-484.

[43] Ruehle S, Remmers F, Romo-Parra H, Massa F, Wickert M, Wörtge S, Häring M, Kaiser N, Marsicano G, Pape HC, Lutz B (2013) Cannabinoid CB1 receptor in dorsal telencephalic glutamatergic neurons: distinctive sufficiency for hippocampus-dependent and amygdala-dependent synaptic and behavioral functions. *J Neurosci* **33**, 10264-10277.

[44] Kash SF, Tecott LH, Hodge C, Baekkeskov S. (1999) Increased anxiety and altered responses to anxiolytics in mice deficient in the 65-kDa isoform of glutamic acid decarboxylase. *Proc Natl Acad Sci USA* **96**,1698–1703.

[45] Herzog E, Gilchrist J, Gras C, Muzerelle A, Ravassard P, Giros B, Gaspar P, El Mestikawy S (2004). Localization of VGLUT3, the vesicular glutamate transporter type 3, in the rat brain. *Neuroscience* **123**, 983-1002.

[46] Harkany T, Härtig W, Berghuis P, Dobszay MB, Zilberter Y, Edwards RH, Mackie K, Ernfors P (2003) Complementary distribution of type 1 cannabinoid receptors and vesicular glutamate transporter 3 in basal forebrain suggests input-specific retrograde signalling by cholinergic neurons. Eur J Neurosci **18**, 1979-1992.

[47] Steindel F, Lerner R, Häring M, Ruehle S, Marsicano G, Lutz B, Monory K (2013) Neuron-type specific cannabinoid-mediated G protein signalling in mouse hippocampus. *J Neurochem* **124**, 795-807.

[48] Katona I, Rancz EA, Acsady L, Ledent C, Mackie K, Hajos N, Freund TF (2001) Distribution of CB1 cannabinoid receptors in the amygdala and their role in the control of GABAergic transmission. *J Neurosci* **21**, 9506-9518.

[49] Almeida-Suhett CP, Prager EM, Pidoplichko V, Figueiredo TH, Marini AM, Li Z, Eiden LE, Braga MF (2014) Reduced GABAergic inhibition in the basolateral amygdala and the development of anxiety-like behaviors after mild traumatic brain injury. *PLoS One* **9**(7).

[50] Müller I, Çalışkan G, Stork O (2015) The GAD65 knock out mouse - a model for GABAergic processes in fear- and stress-induced psychopathology. *Genes Brain Behav* **14**, 37-45.

[51] Roozendaal B, McReynolds JR, Van der Zee EA, Lee S, McGaugh JL, McIntyre CK, (2009) Glucocorticoid effects on memory consolidation depend on functional interactions between the medial prefrontal cortex and basolateral amygdala. *J Neurosci* **29**, 14299 –14308.

[52] Imperatore R, Morello G, Luongo L, Ulrike T, Romano R, De Gregorio D, Belardo C, Maione S, Di Marzo V, Cristino L (2015) Genetic deletion of monoacylglycerol lipase leads to impaired cannabinid receptor CB1R signaling and anxiety-like behavior. *J Neurochem* **135**, 77-813.

[53] Patel S, Hill MN, Cheer JF, Wotjak CT (2017) Holmes, A. The endocannabinoid system as a target for novel anxiolytic drugs. *Neurosci Biobehav Rev* **76(Pt A)**, 56-66.

[54] Malin EL, McGaugh JL (2006) Differential involvement of the hippocampus, anterior cingulate cortex, and basolateral amygdala in memory for context and footshock. *Proc Natl Acad Sci U S A* **103**, 1959-1963.

[55] Nazarinia E, Rezayof A, Sardari M, Yazdanbakhsh N (2017) Contribution of the basolateral amygdala NMDA and muscarinic receptors in rat's memory retrieval. *Neurobiol Learn Mem* **139**, 28-36.

[56] Clinton LK, Billings LM, Green KN, Caccamo A, Ngo J, Oddo S, McGaugh JL, LaFerla FM (2007) Age-dependent sexual dimorphism in cognition and stress response in the 3xTg-AD mice. *Neurobiol Dis* **28**, 76-82.

[57] Aso E, Palomer E, Juvés S, Maldonado R, Muñoz FJ, Ferrer I (2016) CB1 agonist ACEA protects neurons and reduces the cognitive impairment of AβPP/PS1 mice. *J Alzheimers Dis* **30**, 439-459.

[58] Meng ID, Manning BH, Martin WJ, Fields HL (1998) An analgesia circuit activated by cannabinoids. *Nature* **395**, 381-383.

[59] Abush H, Akirav I (2010) Cannabinoids modulate hippocampal memory and plasticity. *Hippocampus* **20**, 1126-1138.

[60] Crowe MS, Leishman E, Banks ML, Gujjar R, Mahadevan A, Bradshaw HB, Kinsey SG (2015) Combined inhibition of monoacylglycerol lipase and cyclooxygenases synergistically reduces neuropathic pain in mice. *Br J Pharmacol* **172**, 1700-1712.

[61] Schlosburg JE, Blankman JL, Long JZ, Nomura DK, Pan B, Kinsey SG, Nguyen PT, Ramesh D, Booker L, Burston JJ, Thomas EA, Selley DE, Sim-Selley LJ Liu QS, Lichtman AH, Cravatt BF (2010) Chronic monoacylglycerol lipase blockade causes functional antagonism of the endocannabinoid system. *Nat Neurosci* **13**, 1113-1119.

[62] Woodhams SG, Chapman V, Finn DP, Hohmann AG, Neugebauer V (2017) The cannabinoid system and pain. *Neuropharmacology* **124**, 105-120.

[63] Vazdarjanova A, McGaugh JL (1999) Basolateral amygdala is involved in modulating consolidation of memory for classical fear conditioning. *J Neurosci* **19**, 6615-6622.

[64] Baeta-Corral R, Defrin R, Pick CG, Giménez-Llort L (2015) Tail-flick test response in 3×Tg-AD mice at early and advanced stages of disease. *Neurosci Lett* **600**,158-163.

[65] Segal M, Auerbach JM (1997) Muscarinic receptors involved in hippocampal plasticity. *Life Sci* **60**, 1085-1091.

[66] Tzavara ET, Bymaster FP, Felder CC, Wade M, Gomeza J, Wess J, McKinzie DL, Nomikos GG (2003) Dysregulated hippocampal acetylcholine neurotransmission and impaired cognition in M2, M4 and M2/M4 muscarinic receptor knockout mice. *Mol Psychiatry* **8**, 673-679.

[67] Levey AI, Edmunds SM, Koliatsos V, Wiley RG, Heilman CJ (1995) Expression of m1-m4 muscarinic acetylcholine receptor proteins in rat hippocampus and regulation by cholinergic innervation. *J Neurosci* **15**, 4077-4092.

[68] Hájos N, Papp EC, Acsády L, Levey AI, Freund TF (1998) Distinct interneuron types express m2 muscarinic receptor immunoreactivity on their dendrites or axon terminals in the hippocampus. *Neuroscience* **82**, 355-376.

Table 1. [^{3}H]CP55,940 binding in different brain areas of seven-month-old Non-Tg and 3xTg-AD mice expressed in fmol/mg t.e. of CB_1 receptors.

	Non-Tg Vehicle	3xTg-AD Vehicle	3xTg-AD WIN55,212-2 [0.1 mg/kg]	3xTg-AD WIN55,212-2 [1 mg/kg]	3xTg-AD JZL184 [8 mg/kg]
Brain region					
Telencephalon					
Amygdala					
Anterior	209 ± 16	269 ± 16	240 ± 20	244 ± 19	209 ± 11
Basolateral	386 ± 12	497 ± 19***	469 ± 20	385 ± 32$	247 ± 14###a,b,c,d
Central	169 ± 6	216 ± 17	190 ± 27	211 ± 24	172 ± 12
Lateral	230 ± 10	253 ± 10	272 ± 29	246 ± 23	182 ± 16#c
Medial	121 ± 8	174 ± 16	155 ± 23	178 ± 24	122 ± 14
Hippocampus					
CA1	593 ± 38	607 ± 28	542 ± 30	473 ± 32	410 ± 25
Oriens	541 ± 36	592 ± 37	584 ± 30	486 ± 18	366 ± 28##b,c
Pyramidal	924 ± 75	909 ± 69	878 ± 42	679 ± 47$	529 ± 56##b,c
Radiatum	603 ± 56	613 ± 51	559 ± 29	482 ± 34	434 ± 44
CA3	591 ± 40	599 ± 19	543 ± 36	496 ± 24	396 ± 27
Oriens	545 ± 51	481 ± 39	499 ± 59	378 ± 32	394 ± 27
Pyramidal	885 ± 70	818 ± 65	763 ± 80	618 ± 67	599 ± 26#a,b
Radiatum	630 ± 89	596 ± 43	591 ± 58	487 ± 59	419 ± 45
Dentate gyrus	473 ± 37	487 ± 17	454 ± 26	434 ± 40	348 ± 22
Granular	922 ± 75	855 ± 49	836 ± 50	711 ± 27	574 ± 35##a,b,c
Molecular	569 ± 55	544 ± 48	489 ± 32	404 ± 30	371 ± 32
Polymorphic	272 ± 25	267 ± 33	224 ± 25	233 ± 19	189 ± 11
Subiculum	861 ± 86	909 ± 38	866 ± 53	712 ± 48	449 ± 56##a,b,c;*d
Cerebral cortex					
Cingular	286 ± 17	316 ± 15	332 ± 25	308 ± 15	247 ± 10#c
Ectorhinal	291 ± 28	321 ± 17	331 ± 32	308 ± 31	220 ± 16#b, c
Entorhinal	254 ± 21	276 ± 18	271 ± 17	254 ± 19	164 ± 12#b, c
Frontal	499 ± 17	427 ± 16	501 ± 22	415 ± 17	310 ± 10##a, c
Motor	340 ± 8	314 ± 13	347 ± 24	317 ± 20	241 ± 11##a, c; #b, d
Perirhinal	278 ± 32	302 ± 9	280 ± 23	271 ± 32	195 ± 13*b
Rhinencephalon					
Lat. olf. tract N	281 ± 40	424 ± 38*	389 ± 32	327 ± 22	239 ± 17##b,#c
Glom. olf. bulb	470 ± 8	304 ± 9***	293 ±15	308 ± 19	276 ± 12###

Data are expressed as mean ± SEM (n = 7 per group) and analyzed by one-way ANOVA, followed by Bonferroni´s *post hoc* test for multiple comparisons. *p < 0.05, ***p < 0.001 *vs* Non-Tg (vehicle). #p < 0.05, ##p < 0.01, ###p < 0.001 *vs* Non-Tg (vehicle) (**a**); 3xTg-AD (vehicle) (**b**); 3xTg-AD (0.1 mg/kg WIN55,212-2) (**c**); 3xTg-AD (1 mg/kg WIN55,212-2) (**d**). $p < 0.05 *vs* 3xTg-AD (vehicle).

Table 2. [^{35}S]GTPγS binding in different brain areas of seven-month-old Non-Tg and 3xTg-AD mice evoked by WIN55,212-2 (10 μM) expressed as percentage of stimulation over the basal binding.

	Non-Tg Vehicle	3xTg-AD Vehicle	3xTg-AD WIN55,212-2 [0.1 mg/kg]	3xTg-AD WIN55,212-2 [1 mg/kg]	3xTg-AD JZL184 [8 mg/kg]
Brain region					
Telencephalon					
Amygdala					
Anterior	82 ± 16	79 ± 16	68 ± 14	98 ± 16	89 ± 24
Basolateral	168 ± 24	281 ± 41*	311 ± 42	213 ± 25	191 ± 31
Central	76 ± 28	61 ± 14	66 ± 17	58 ± 19	63 ± 21
Lateral	156 ± 26	197 ± 36	167 ± 45	159 ± 26	123 ± 23
Medial	35 ± 13	56 ± 9	100 ± 15	77 ± 20	89 ± 20
Hippocampus					
CA1	114 ± 17	63 ± 13	64 ± 6	61 ± 9.9	59 ± 8
Oriens	183 ± 40	164 ± 14	132 ± 11	178 ± 16	110 ± 19
Pyramidal	142 ± 23	165 ± 49	157 ± 15	151 ± 20	112 ± 22
Radiatum	144 ± 32	141 ± 34	105 ± 16	109 ± 16	53 ± 7#
CA3	154 ± 14	104 ± 19	105 ± 11	96 ± 15	116 ± 25
Oriens	143 ± 18	161 ± 17	134 ± 21	143 ± 16	121 ± 21
Pyramidal	94 ± 21	117 ± 22	135 ± 25	141 ± 23	82 ± 13
Radiatum	189 ± 51	123 ± 35	94 ± 19	89 ± 13	93 ± 13
Dentate gyrus	119 ± 17	70 ± 8	65 ± 8	62 ± 10	68 ± 12
Granular	293 ± 71	143 ± 20	193 ± 12	186 ± 36	152 ± 25
Molecular	199 ± 34	108 ± 18*	99 ± 13	113 ± 8	112 ± 20
Polymorphic	261 ± 24	146 ± 20	104 ± 14	134 ± 13	112 ± 13
Ventral subiculum	162 ± 37	130 ± 21	106 ± 15	125 ± 18	127 ± 19
Cerebral cortex					
Cingular	90 ± 10	110 ± 14	102 ± 14	98 ± 10	69 ± 7
Ectorhinal	159 ± 37	131 ± 12	141 ± 21	115 ± 25	93 ± 19
Entorhinal	154 ± 27	165 ± 36	135 ± 22	180 ± 17	149 ± 20
Frontal	101 ± 14	114 ± 20	99 ± 13	115 ± 17	107 ± 15
Motor	108 ± 10	127 ± 18	93 ± 17	88 ± 6	87 ± 5
Perirhinal	168 ± 41	146 ± 29	127 ± 21	107 ± 21	85 ± 12
Striatum	134 ± 19	81 ± 8*	80 ± 6	102 ± 10	73 ± 13
Rhinencephalon					
Lat. olf. tract N	221 ± 58	232 ± 71	230 ± 44	325 ± 61	326 ± 60
Glom. olf. bulb	580 ± 61	343 ± 18**	317 ± 41	391 ± 50	331 ± 22

Data are expressed as mean ± SEM (n = 7 per group) and analyzed by one-way ANOVA, followed by Bonferroni´s *post hoc* test for multiple comparisons. *p < 0.05 *vs* Non-Tg-vehicle; **p < 0.01 *vs* Non-Tg (vehicle). #p < 0.05 *vs* 3xTg-AD (vehicle).

Table 3. [^{35}S]GTPγS binding in different brain areas of seven-month-old Non-Tg and 3xTg-AD mice evoked by carbachol (100 μM) expressed as percentage of stimulation over the basal binding.

	Non-Tg Vehicle	3xTg-AD Vehicle	3xTg-AD WIN55.212-2 [0.1 mg/kg]	3xTg-AD WIN55.212-2 [1 mg/kg]	3xTg-AD JZL184 [8 mg/kg]
Brain region					
Telencephalon					
Amygdala					
Anterior	89 ± 18	92 ± 21	128 ± 20	116 ± 10	82 ± 17
Basolateral	102 ± 14	55 ± 10*	68 ± 16	97 ± 12#	71 ± 11
Central	43 ± 7	31 ± 9	40 ± 8	43 ± 6	53 ± 15
Lateral	96 ± 18	41 ± 11*	43 ± 12	84 ± 9##	55 ± 8
Medial	66 ± 6	49 ± 14	31 ± 7	54 ± 10	46 ± 11
Hippocampus					
CA1	42 ± 7	21 ± 3*	38 ± 8	39 ± 12	28 ± 8
Oriens	33 ± 7	29 ± 9	36 ± 8	59 ± 11	26 ± 9
Pyramidal	30 ± 6	16 ± 7*	23 ± 6	34 ± 7	14 ± 5
CA3	43 ± 9	33 ± 6	43 ± 5	47 ± 15	46 ± 9
Oriens	30 ± 12	24 ± 10	27 ± 8	49 ± 12	27 ± 4
Pyramidal	34 ± 14	29 ± 5	28 ± 10	53 ± 15	33 ± 7
Dentate gyrus	34 ± 8	21 ± 5	28 ± 6	21 ± 5	21 ± 4
Granular	23 ± 9	26 ± 9	32 ± 10	19 ± 6	21 ± 6
Molecular	21 ± 6	19 ± 4	16 ± 13	17 ± 4	8 ± 3
Polymorphic	16 ± 15	24 ± 5	3 ± 12	23 ± 13	11 ± 6
Cerebral cortex					
Cingular	62 ± 12	64 ± 13	54 ± 10	68 ± 11	58 ± 9
Ectorhinal	39 ± 15	42 ± 12	38 ± 13	46 ± 9	37 ± 5
Entorhinal	41 ± 13	30 ± 14	27 ± 9	37 ± 11	34 ± 9
Frontal	54 ± 18	57 ± 12	42 ± 9	68 ± 12	57 ± 10
Motor	59 ± 11	56 ± 12	50 ± 11	59 ± 11	46 ± 8
Perirhinal	46 ± 7	40 ± 5	43 ± 10	45 ± 5	51 ± 12
Rhinencephalon					
Lat. olf. tract N	173 ± 22	107 ± 16*	125 ± 14	140 ± 20	112 ± 8
Glom. olf. bulb	193 ± 26	295 ± 15*	312 ± 45	279 ± 54	266 ± 38

Data are expressed as mean ± SEM (n = 7 per group) and analyzed by one-way ANOVA, followed by Bonferroni´s *post hoc* test for multiple comparisons. *$p < 0.05$ *vs* Non-Tg (vehicle). #$p < 0.05$; ##$p < 0.01$ *vs* 3xTg-AD (vehicle).

Figure captions

Figure 1. Synopsis of the experimental design including treatment schedule and behavioral assessment.

Figure 2. Passive avoidance test and CB_1 receptor binding sites. (A) Acquisition latency times during the learning trial in both genotypes in the absence of treatment; **p < 0.01 *vs* Non-Tg. (B) Step-through latency times in both genotypes represented as Kaplan-Meier survival curves. (C) 3xTg-AD mice treated with different cannabinoid agonists. The subchronic administration of WIN55,212-2 (1 mg/kg) and JZL184 (8 mg/kg) for seven consecutive days triggered a statistically significant decrease in the acquisition latency compared to that obtained in the Non-Tg group; * p < 0.05 *vs* 3xTg-AD mice treated with vehicle. (D) Step-through latency times in 3xTg-AD mice represented as Kaplan-Meier survival curves. The probability is plotted over the step-through latency in 3xTg-AD mice after different cannabinoid-based treatments. Acquisition latencies were analyzed by a one-way ANOVA, followed by Bonferroni´s *post hoc* test for multiple comparisons. The step-through latencies were represented as Kaplan-Meier survival curves, and for comparisons the nonparametric Log-rank/Mantel-Cox test was used (n = 9-10 mice/group). (E) [^{3}H]CP55,940 binding autoradiography in representative brain coronal sections from both genotypes treated with vehicle and from 3xTg-AD treated with either WIN55,212-2 (1 mg/kg) or JZL184 (8 mg/kg). Note that both pharmacological treatments decreased the density of receptors in the whole grey matter including the basolateral amygdala (BLA) (boxed area). [^{3}H]-microscales used as standards in µCi/g t.e. Scale bar: 5 mm.

Figure 3. [^{3}H]CP55,940 binding autoradiography in brain and spleen. The image shows the cannabinoid receptor distribution in brain and spleen samples from 3xTg-

AD, CB_1 receptor knockout ($CB_1^{-/-}$) and wild type ($CB_1^{+/+}$) mice. The total binding is shown in the top row, displaying the characteristic and well-described distribution of cannabinoid receptors in the brain, and surrounding the lymphatic nodules (white pulp) in the spleen. In the presence of 0.1 μ M of SR141716A, a CB_1 receptor specific antagonist, binding is almost completely blocked in the brain but not in the spleen (middle row) while 0.1 μM of SR144528, a CB_2 receptor specific antagonist, completely displaced the [^{3}H]CP55,940 binding in the spleen without affecting the binding in the brain (bottom row). Note the absence of binding in the brain from $CB_1^{-/-}$ and the identical distribution in the spleen from both Non-Tg and knockout mice, revealing the preponderance of CB_1 receptors in the brain and CB_2 receptors in spleen tissue, and the specificity of the cannabinoid antagonists. Scale bar = 5 mm.

Figure 4. [^{35}S]GTPγS autoradiography. [^{35}S]GTPγS binding evoked by both WIN55,212-2 (10 μM) for cannabinoid receptors (A-D) and carbachol (100 μM) for M_2/M_4 muscarinic acetylcholine receptors (mAChR) (E-H), in representative coronal brain sections from Non-Tg and 3xTg-AD mice treated with vehicle and cannabinoid agonists. The highest CB_1 receptor stimulation was found in the hippocampus, the most caudal portion of the globus pallidus, the deeper layers of the cortex, and the amygdaloid complex. Thus, in the amygdala, the latero-basolateral region (boxed area) (A-D) seems to be the most activated, displaying a hyperactivation in 3xTg-AD (B) mice, which is attenuated with both cannabinoids (C-D). Moreover, deregulation of mAChR functionality in 3xTg-AD mice was found. Note the decrease in the latero-basolateral region and in the pyramidal layer of the hippocampal CA1 region (boxed areas) (F) and the potentiation of muscarinic signaling in the amygdala following the subchronic administration of 1 mg/kg of WIN55,212-2 (G). [^{14}C]-microscales used as standards in μCi/g t.e. Scale bar: 5 mm.

Figure 5. CB_1 receptor-mediated signaling and behavior. [^{3}H]CP55,940 binding in the BLA in both genotypes treated with vehicle (A) and in 3xTg-AD mice treated with WIN55,212-2 (0.1 mg/kg or 1 mg/kg) or JZL184 (8 mg/kg) (B). Correlation analyses between the CB_1 receptor density in the BLA and the acquisition latency times of both genotypes (C) and of 3xTg-AD mice after cannabinoid treatments (D). Note that data are grouped according to both, genotype and treatment.

Quantification of CB_1 receptor stimulation (% over basal activity) evoked by WIN55,212-2 (10 µM) in the BLA of both genotypes (E) and of 3xTg-AD mice treated with WIN55,212-2 (0.1 mg/kg or 1 mg/kg) or JZL184 (8 mg/kg) (F). Correlation analyses between the endocannabinoid signaling in the BLA and the acquisition latency times of both genotypes (G) and of 3xTg-AD mice after cannabinoid treatments (H). Note that data are grouped according to genotype and not to treatment.). Data are expressed as mean ± SEM (n = 7 per group), and analyzed by a one-way ANOVA, followed by Bonferroni´s *post hoc* test for multiple comparisons. *p < 0.05; **p < 0.01 and ***p < 0.001. Behavioral correlations with neurochemical data were analyzed with Pearson's correlation.

Figure 6. Localization of CB_1 receptors in the BLA. Double labeling of tissue sections including the amygdaloid complex from seven-month-old 3xTg-AD mice processed for CB_1 receptor (in green) and vesicular glutamate transporter type 3 (VGLUT3) (A2 and C2 in red) as a glutamatergic marker, and glutamic acid decarboxylase isoform 65kDa (GAD65) (B2 and D2 in red) as a GABAergic presynaptic marker. The different amygdaloid nuclei exhibited specific CB_1 receptor-immunostaining patterns. VGLUT3 was distributed presumably in postsynaptic somatodendritic compartment (A2 and C2) while GAD65 immunostaining was clearly delineated presynaptic inhibitory boutons (B2 and D2). In low magnification images, note the distribution of CB_1 receptors surrounding positive glutamatergic neurons (A3)

and sharing localization with GAD65 (B3); scale bar: 150 µ m. High magnification images showed the intracellular localization of VGLUT3 (C2) closely surrounding the nuclei stained with Hoechst (C3 in blue) revealing the almost complete lack of colocalization with CB_1 receptors (C4). Conversely, CB_1 receptors were located on GAD65-positive terminals (D4), revealing its presynaptic localization on inhibitory synaptic boutons. Scale bar = 10 µm. Bregma -1.82 mm. CeL central amygdaloid nucleus, lateral division; La lateral amygdaloid nucleus; BLA basolateral amygdaloid nucleus, anterior part; BLP basolateral amygdaloid nucleus, posterior part; BMP basomedial amygdaloid nucleus, posterior part.

Figure 7. Localization of M_2 mAChR in the hippocampus. Double labeling of tissue sections including the CA1 field of the hippocampus from a representative seven-month-old 3xTg-AD mouse processed for M_2 mAChR (in red) and VGLUT3 (A2 and C1 in green) as a glutamatergic marker, and GAD65 (B2 and D1 in green) as a GABAergic presynaptic marker. The different hippocampal subfields exhibited specific M_2 mAChR-immunostaining patterns delineating the perikarya of the large pyramidal neurons in basket-like formations. VGLUT3 was distributed near the nucleus (A2 and C1), presumably in the somatodendritic compartment of pyramidal neurons, while GAD65 immunostaining (B2 and D1) clearly delineated presynaptic inhibitory boutons. In low magnification images, note the complementary distribution of M_2 mAChR-immunoreactivity to VGLUT3, surrounding the pyramidal neurons (A3), and the localization in GAD65-positive presynaptic terminals (B3); scale bar: 150 µm. High magnification images revealed the intracellular localization of VGLUT3 (C1) closely surrounding the nuclei stained with Hoechst (C3 in blue) and the almost complete lack of colocalization with M_2 mAChR (C4). Conversely, M_2 mAChR were distributed in GAD65-positive terminals, revealing the presynaptic localization on inhibitory synaptic boutons (D4). Scale bar = 10 µm. Bregma -3.08 mm. Alv alveus of the hippocampus;

Or oriens layer of the hippocampus; Py pyramidal cell layer of the hippocampus; Rad radiatum layer of the hippocampus; LMol lacunosum molecular layer of the hippocampus.

Figure 1

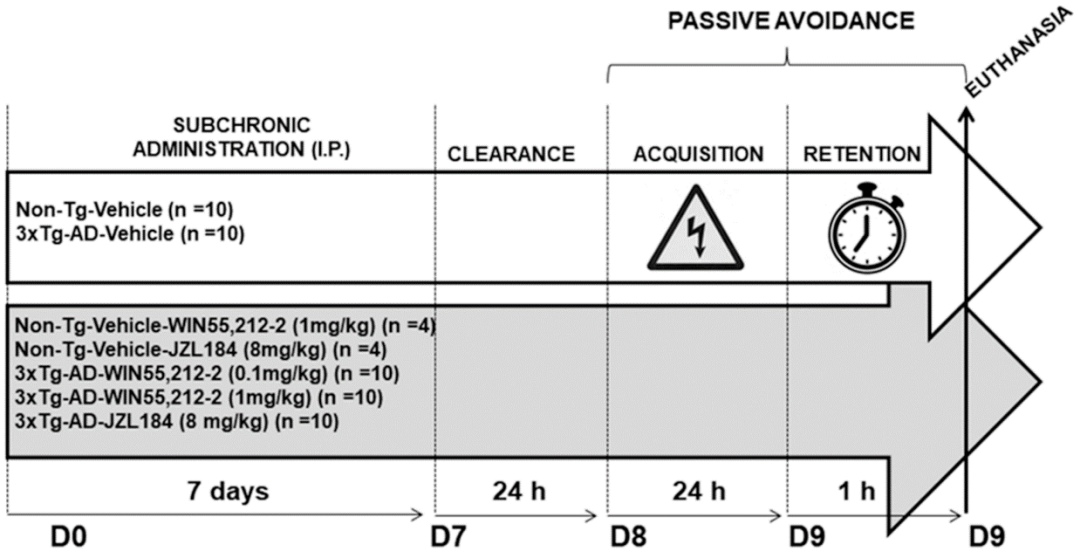
PASSIVE AVOIDANCE
EUTHANASIA
SUBCHRONIC ADMINISTRATION (I.P.)
CLEARANCE
ACQUISITION
RETENTION
Non-Tg-Vehicle (n =10)
3xTg-AD-Vehicle (n =10)
Non-Tg-Vehicle-WIN55,212-2 (1mg/kg) (n =4)
Non-Tg-Vehicle-JZL184 (8mg/kg) (n =4)
3xTg-AD-WIN55,212-2 (0.1mg/kg) (n =10)
3xTg-AD-WIN55,212-2 (1mg/kg) (n =10)
3xTg-AD-JZL184 (8 mg/kg) (n =10)
7 days
24 h
24 h
1 h
D0
D7
D8
D9
D9

Figure 2

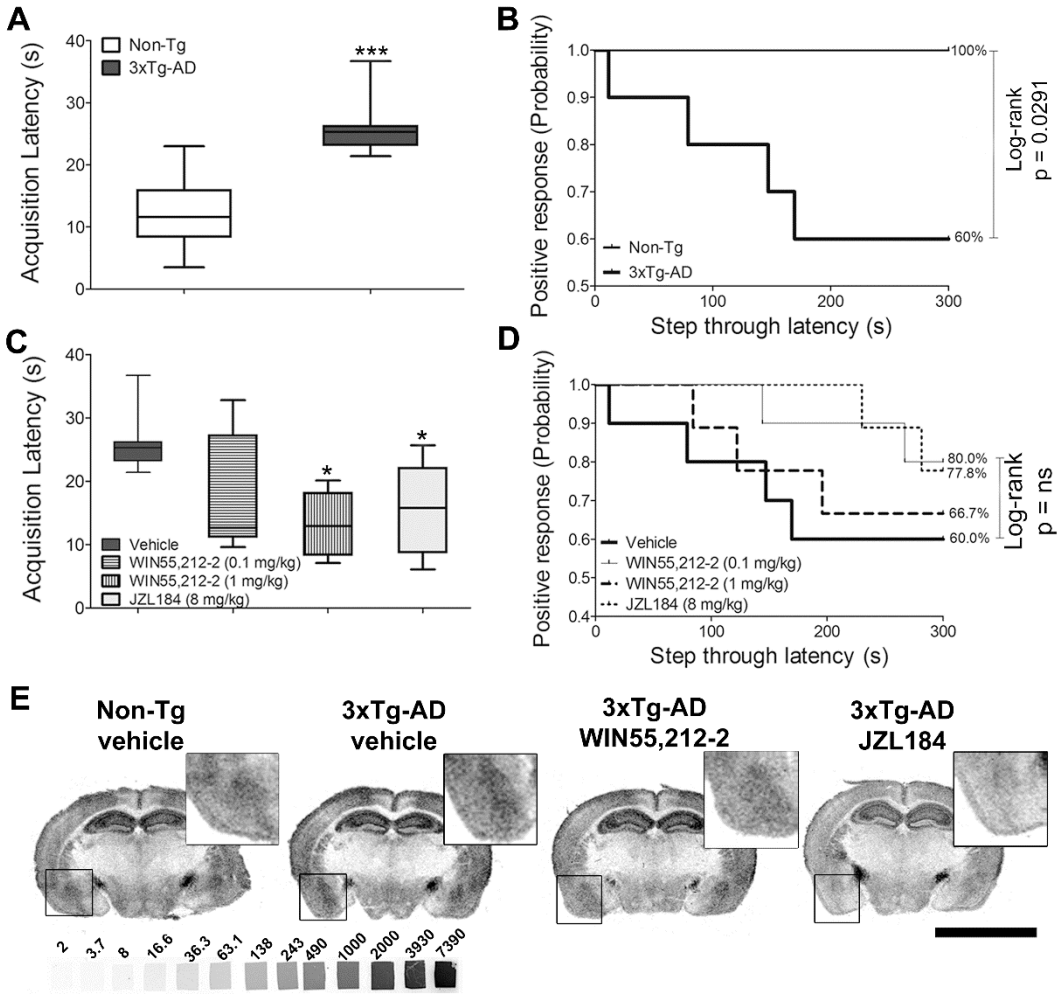
A
Non-Tg
3xTg-AD
***
Acquisition Latency (s)
B
Positive response (Probability)
100%
60%
Log-rank
p = 0.0291
Non-Tg
3xTg-AD
Step through latency (s)
C
Acquisition Latency (s)
*
*
Vehicle
WIN55,212-2 (0.1 mg/kg)
WIN55,212-2 (1 mg/kg)
JZL184 (8 mg/kg)
D
Positive response (Probability)
80.0%
77.8%
66.7%
60.0%
Log-rank
p = ns
Vehicle
WIN55,212-2 (0.1 mg/kg)
WIN55,212-2 (1 mg/kg)
JZL184 (8 mg/kg)
Step through latency (s)
E
Non-Tg
vehicle
3xTg-AD
vehicle
3xTg-AD
WIN55,212-2
3xTg-AD
JZL184
2
3.7
8
16.6
36.3
63.1
138
243
490
1000
2000
3930
7390

Figure 3

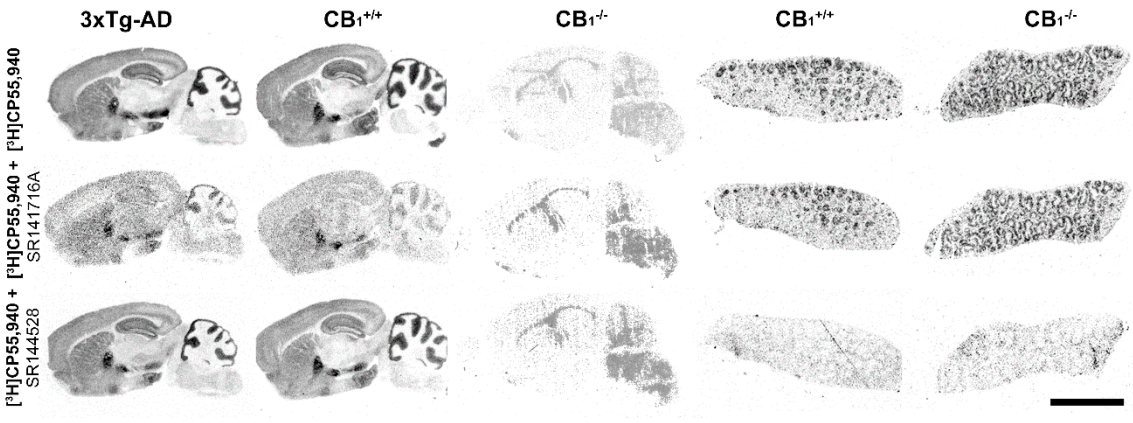
3xTg-AD
CB1+/+
CB1-/-
CB1+/+
CB1-/-
[3H]CP55,940
[3H]CP55,940 + SR141716A
[3H]CP55,940 + SR144528

Figure 4

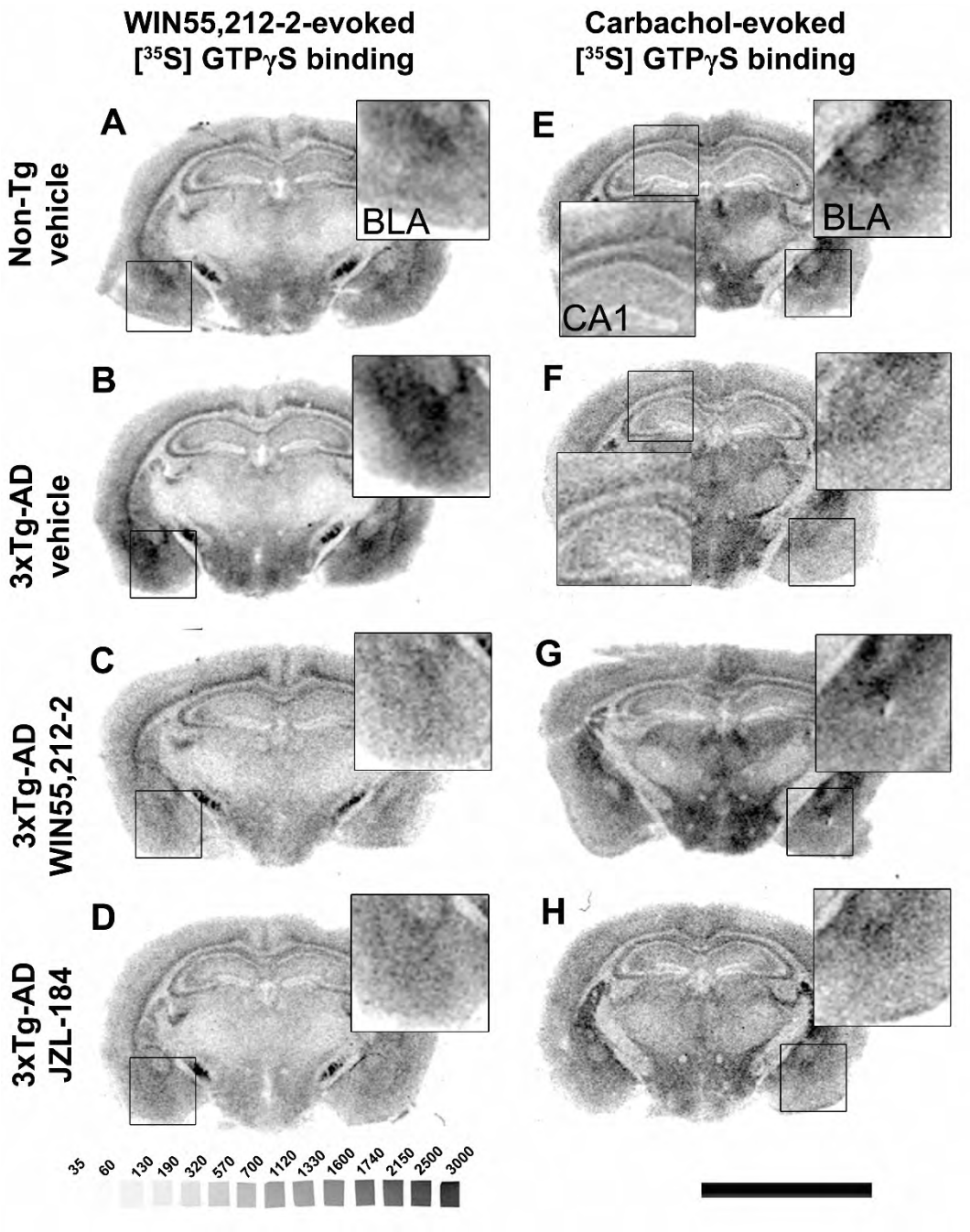
WIN55,212-2-evoked
[35S] GTPγS binding
Carbachol-evoked
[35S] GTPγS binding
A
E
BLA
BLA
CA1
Non-Tg
vehicle
B
F
3xTg-AD
vehicle
C
G
3xTg-AD
WIN55,212-2
D
H
3xTg-AD
JZL-184
35
60
130
190
320
570
700
1120
1330
1600
1740
2150
2500
3000

Figure 5

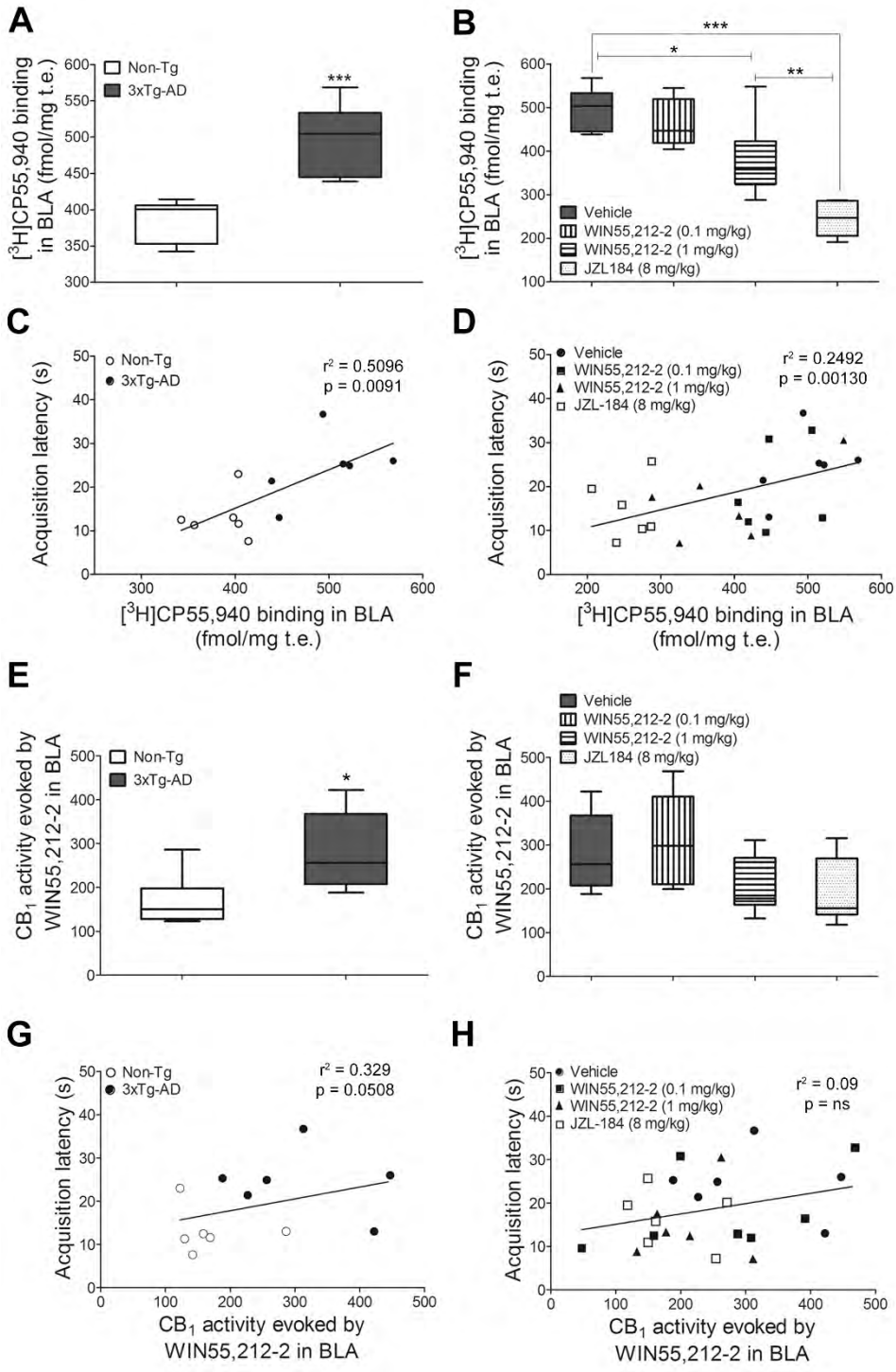
A
Non-Tg
3xTg-AD
***
[3H]CP55,940 binding in BLA (fmol/mg t.e.)
B
***
*
**
Vehicle
WIN55,212-2 (0.1 mg/kg)
WIN55,212-2 (1 mg/kg)
JZL184 (8 mg/kg)
C
Non-Tg
3xTg-AD
r2 = 0.5096
p = 0.0091
Acquisition latency (s)
[3H]CP55,940 binding in BLA (fmol/mg t.e.)
D
Vehicle
WIN55,212-2 (0.1 mg/kg)
WIN55,212-2 (1 mg/kg)
JZL-184 (8 mg/kg)
r2 = 0.2492
p = 0.00130
E
Non-Tg
3xTg-AD
*
CB1 activity evoked by WIN55,212-2 in BLA
F
G
Non-Tg
3xTg-AD
r2 = 0.329
p = 0.0508
H
Vehicle
WIN55,212-2 (0.1 mg/kg)
WIN55,212-2 (1 mg/kg)
JZL-184 (8 mg/kg)
r2 = 0.09
p = ns

Figure 6

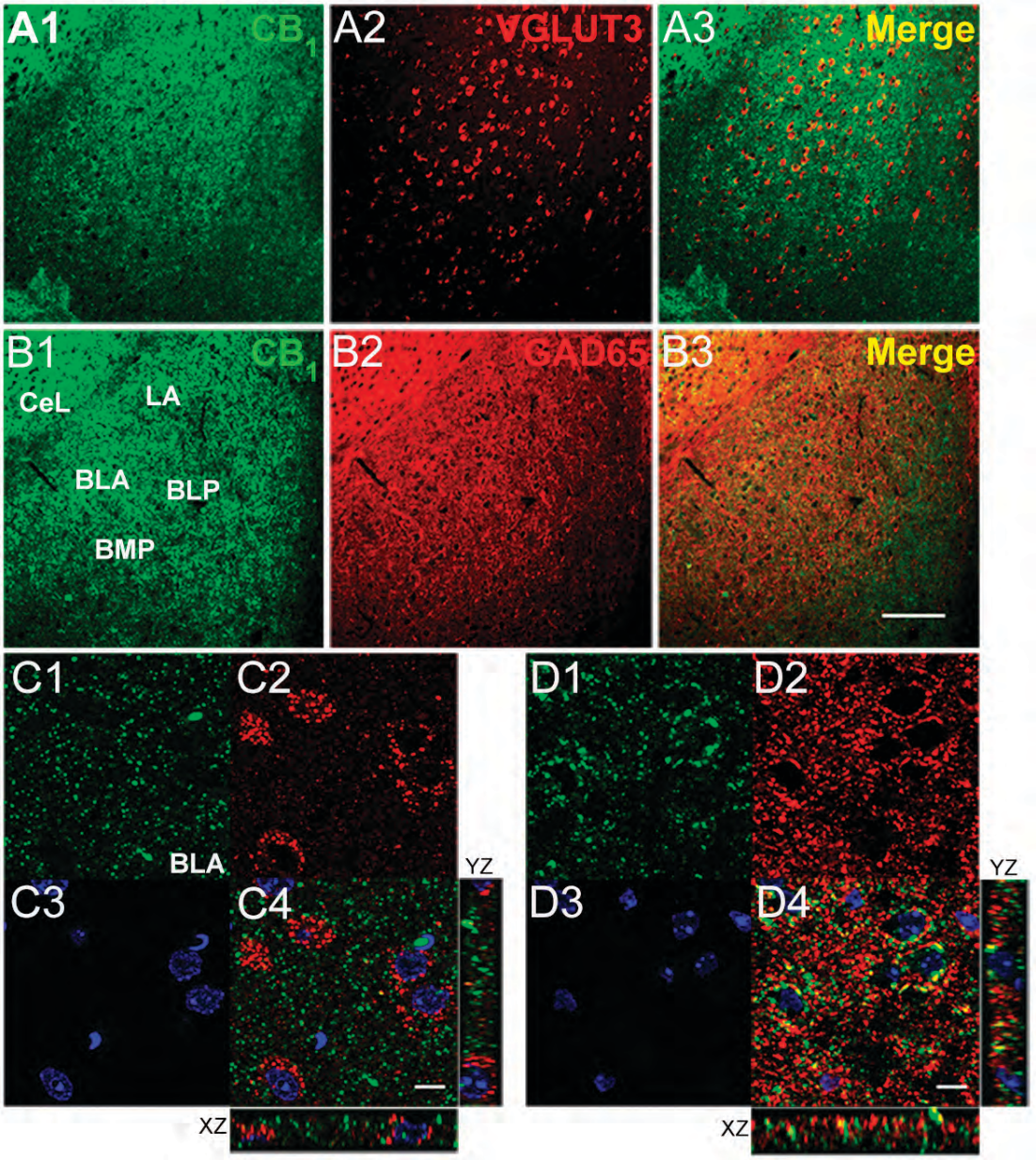
A1
CB1
A2
VGLUT3
A3
Merge
B1
CB1
CeL
LA
BLA
BLP
BMP
B2
GAD65
B3
Merge
C1
C2
BLA
C3
C4
YZ
XZ
D1
D2
D3
D4
YZ
XZ

Figure 7

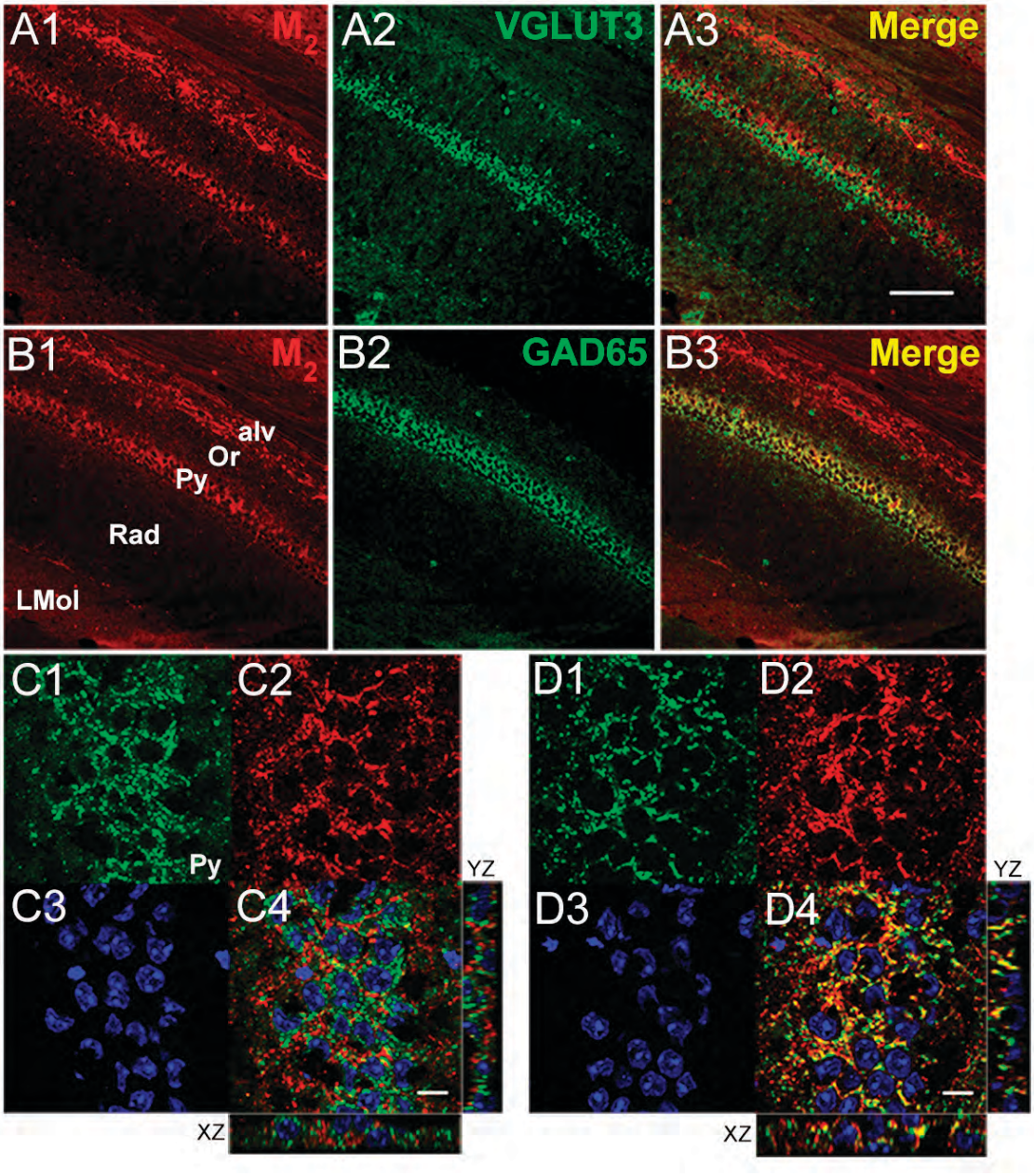
A1
M2
A2
VGLUT3
A3
Merge
B1
M2
alv
Or
Py
Rad
LMol
B2
GAD65
B3
Merge
C1
C2
Py
YZ
C3
C4
XZ
D1
D2
YZ
D3
D4
XZ

Supplementary *tables*

Supplementary Table 1. [^{3}H]CP55,940 binding in different brain areas of seven-month-old Non-Tg and 3xTg-AD mice expressed in fmol/mg t.e. of CB_1 receptors.

	Non-Tg Vehicle	3xTg-AD Vehicle	3xTg-AD WIN55,212-2 [0.1 mg/kg]	3xTg-AD WIN55,212-2 [1 mg/kg]	3xTg-AD JZL184 [8 mg/kg]
Brain region					
Grey matter					
Telencephalon					
Cerebral cortex					
Piriform	229 ± 9	216 ± 22	235 ± 20	248 ± 25	193 ± 10
Somatosensory	204 ± 21	220 ± 18	241 ± 23	254 ± 23	211 ± 10
Mesencephalon					
Globus pallidus	1950 ± 137	1708 ± 123	1805 ± 83	1425 ± 102	1756 ± 142
Striatum	461 ± 44	376 ± 36	384 ± 18	359 ± 17	282 ± 29
Nucleus basalis	246 ± 14	251 ± 19	276 ± 23	291 ± 15	196 ± 14$^{\#a,b,c,d}$
Sustantia nigra	2034 ± 145	1830 ± 109	1761 ± 51	1692 ± 83	1631 ± 49
White matter					
Corpus callosum	55 ± 13	76 ± 15	75 ± 14	116 ± 18	84 ± 12
Fimbria fornix	56 ± 7	98 ± 12	103 ± 15	140 ± 12	79 ± 7
Internal capsule	-5 ± 12	17 ± 10	24 ± 16	38 ± 10	11 ± 5
Lateral olf tract	195 ± 28	237 ± 27	227 ± 20	255 ± 20	184 ± 15
Optic tract	12 ± 13	33 ± 27	60 ± 25	60 ± 17	31 ± 10
Lac moleculare	678 ± 83	637 ± 70	592 ± 50	472 ± 66	394 ± 54

Data are expressed as mean ± SEM (n = 7 per group), and analyzed by a one-way ANOVA, followed by Bonferroni´s *post hoc* test for multiple comparisons. $^{\#}p < 0.05$, compared with Non-Tg (vehicle) (**a**); 3xTg-AD (vehicle) (**b**); 3xTg-AD (0.1 mg/kg WIN55,212-2) (**c**); 3xTg-AD (1 mg/kg WIN55,212-2) (**d**).

Supplementary Table 2. [^{35}S]GTPγS binding in different brain areas of seven-month-old Non-Tg and 3xTg-AD mice evoked by WIN55,212-2 (10 μ M) expressed as percentage of stimulation over the basal binding.

	Non-Tg Vehicle	3xTg-AD Vehicle	3xTg-AD WIN55,212-2 [0.1 mg/kg]	3xTg-AD WIN55,212-2 [1 mg/kg]	3xTg-AD JZL184 [8 mg/kg]
Brain region					
Grey matter					
Telencephalon					
Cerebral cortex					
Piriform	89 ± 18	71 ± 9	74 ± 9	91 ± 21	70 ± 6
Somatosensory	62 ± 9	68 ± 8	51 ± 13	59 ± 9	66 ± 9
Diencephalon					
Nucleus basalis	130 ± 26	112 ± 18	104 ± 9	121 ± 15	97 ± 12
Mesencephalon					
Globus pallidus	1188 ± 157	1161 ± 116	1026 ± 73	1114 ± 56	1057 ± 85
Sustantia nigra	1974 ± 181	1781 ± 166	1541 ± 111	1595 ± 97	1356 ± 91
White matter					
Corpus callosum	5 ± 9	11 ± 5	11 ± 7	12 ± 14	23 ± 5
Fimbria fornix	96 ± 8	40 ± 12	42 ± 5	48 ± 16	52 ± 12
Internal capsule	50 ± 17	1 ± 7	20 ± 14	19 ± 9	21 ± 7
Lateral olfact tract	90 ± 32	63 ± 26	76 ± 25	70 ± 13	86 ± 6
Optic tract	28 ± 27	24 ± 11	57 ± 21	31 ± 12	34 ± 8
Lacunosum moleculare	132 ± 27	135 ± 34	88 ± 15	108 ± 15	92 ± 19

Data are expressed as mean ± SEM (n = 7 per group) and analyzed by a one-way ANOVA, followed by Bonferroni´s *post hoc* test for multiple comparisons.

Supplementary Table 3. [^{35}S]GTPγS binding in different brain areas of seven-month-old Non-Tg and 3xTg-AD mice evoked by carbachol (100 μM) expressed as percentage of stimulation over the basal binding.

	Non-Tg Vehicle	3xTg-AD Vehicle	3xTg-AD WIN55.212-2 [0.1 mg/kg]	3xTg-AD WIN55.212-2 [1 mg/kg]	3xTg-AD JZL184 [8 mg/kg]
Brain region					
Grey matter					
Telencephalon					
Cerebral cortex					
Piriform	45 ± 11	77 ± 24	73 ± 14	41 ± 5	28 ± 8
Somatosensory	69 ± 16	54 ± 10	60 ± 12	55 ± 12	43 ± 8
Diencephalon					
Nucleus basalis	82 ± 17	99 ± 22	112 ± 11	96 ± 23	70 ± 14
Mesencephalon					
Globus pallidus	35 ± 8	27 ± 8	35 ± 9	25 ± 7	39 ± 8
Striatum	161 ± 18	125 ± 25	127 ± 12	142 ± 11	119 ± 23
Sustantia nigra	51 ± 17	44 ± 8	45 ± 5	43 ± 6	44 ± 9
White matter					
Corpus callosum	42 ± 9	57 ± 17	53 ± 12	55 ± 11	41 ± 6
Fimbria fornix	62 ± 11	46 ± 8	62 ± 11	57 ± 8	45 ± 6
Internal capsule	35 ± 10	8 ± 7	35 ± 10	21 ± 8	27 ± 8
Lateral olfactory tract	55 ± 16	59 ± 12	49 ± 9	60 ± 12	51 ± 7
Optic tract	35 ± 5	22 ± 6	33 ± 17	44 ± 10	29 ± 14

Data are expressed as mean ± SEM (n = 7 per group) and analyzed by a one-way ANOVA, followed by Bonferroni´s *post hoc* test for multiple comparisons.

Supplementary Figure

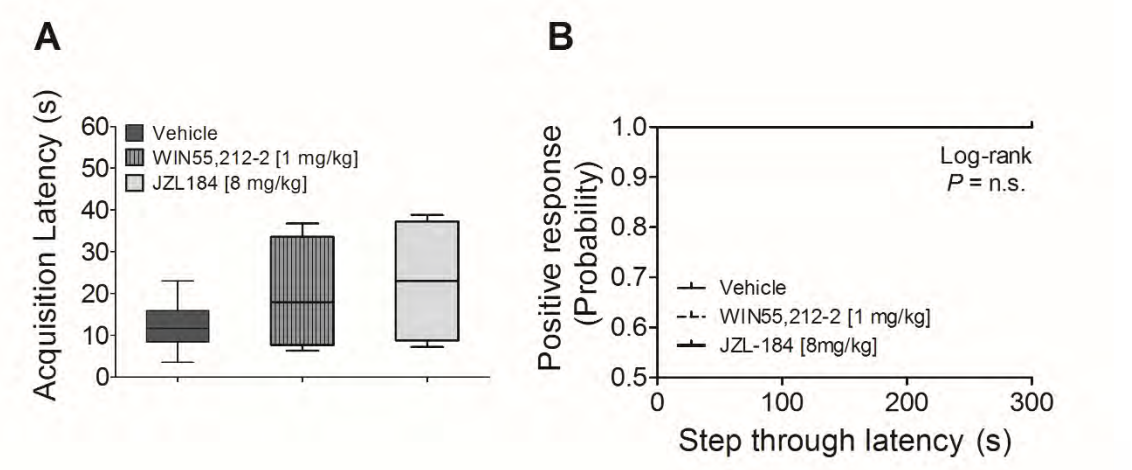

Passive avoidance test in Non-Tg mice following cannabinoid treatment. (A) Acquisition latency times during the learning trial in Non-Tg mice treated with vehicle (n = 10) or cannabinoid agonists (WIN55,212-2, n = 4 and JZL184, n = 4). Data are expressed as mean ± SEM (n = 7 per group) and analyzed by a one-way ANOVA, followed by Bonferroni´s *post hoc* test for multiple comparisons. (B) Step-through latency times in Non-Tg represented as Kaplan-Meier survival curves in the same groups. Note that the subchronic administration of cannabinoids did not modify either of both parameters.